Global C-Band Envisat and Sentinel-1 SAR measurements in co- and cross-polarization
-
Global Ku- and Ka- near nadir measurements from Global Precipitation Measurements mission

Elements for discussion & Focus on Sea-Ice

A. Mouche, IFREMER/LOS

B. Chapron, F. Paul, J. Tournadre, F. Girard-Ardhuin & P. Queffeulou, IFREMER/LOS
N. Longépé, CLS/DAR
W. Alpers, UH
H. Johnsen, Norut
F. Collard & G. Guitton, ODL
F. Nouguier, MIO

- General Approach

  Maximize the use of satellite observations to

  - Improve our understanding of electromagnetic and oceanic waves interactions

  - Document and describe air-sea interface interactions

- Context

  - International Earth Observation Programme

The Co-polarization Quest

- Opportunity to get massive co-locations with ASCAT winds and NRCS from ENVISAT (<1h)

  ➡ Direct description of NRCS behavior in VV and HH at C-Band from space for the first time

- 2700 co-located WSM images
- 150 000 and 250 000 co-locations points for VV and HH
- Incidence angles between 16 to 42 degrees
- Wind speeds range from 2 to 22 m/s

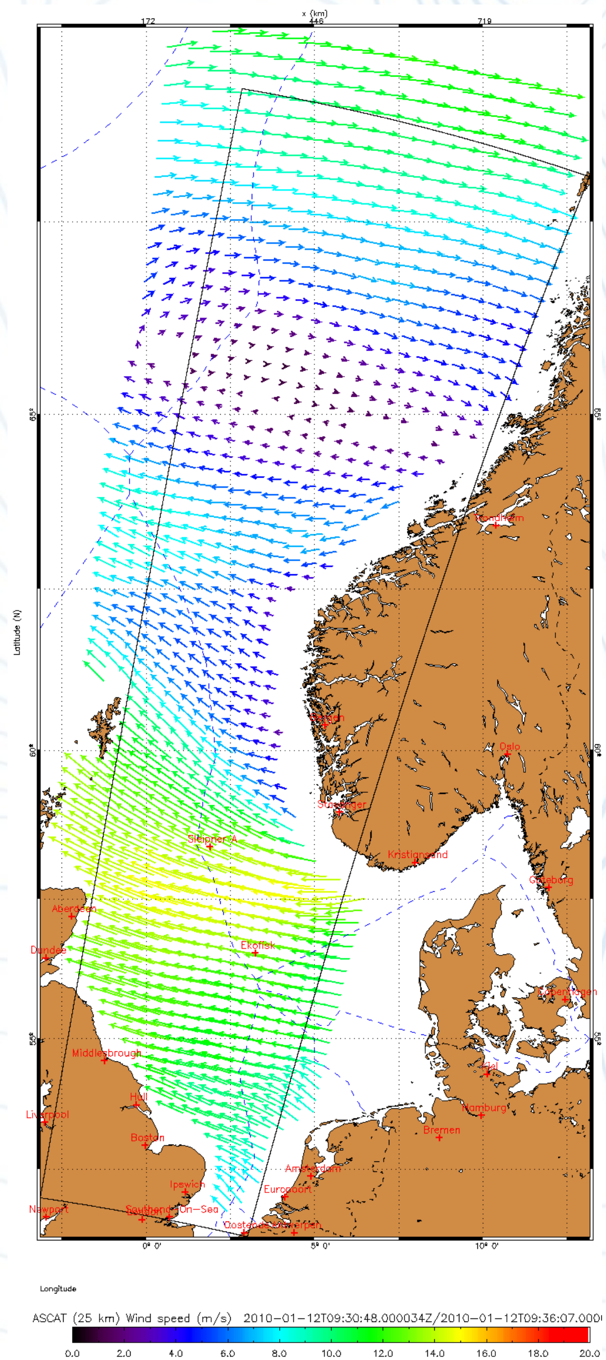

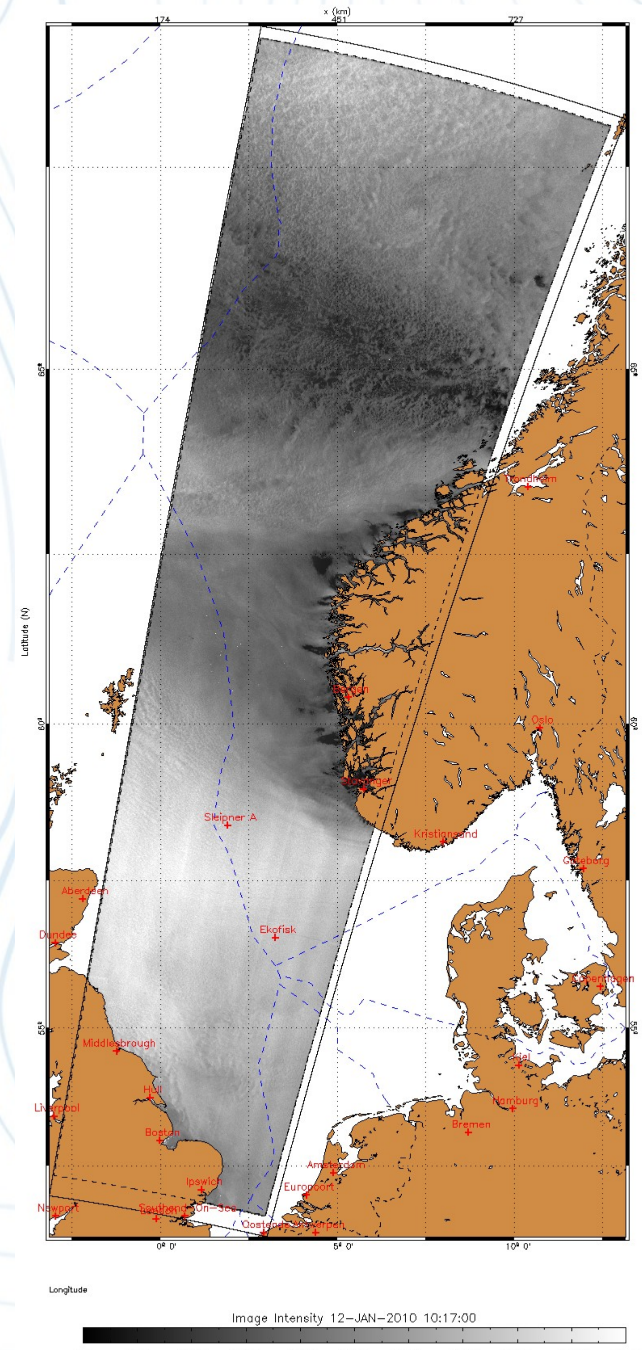

The Co-polarization Quest

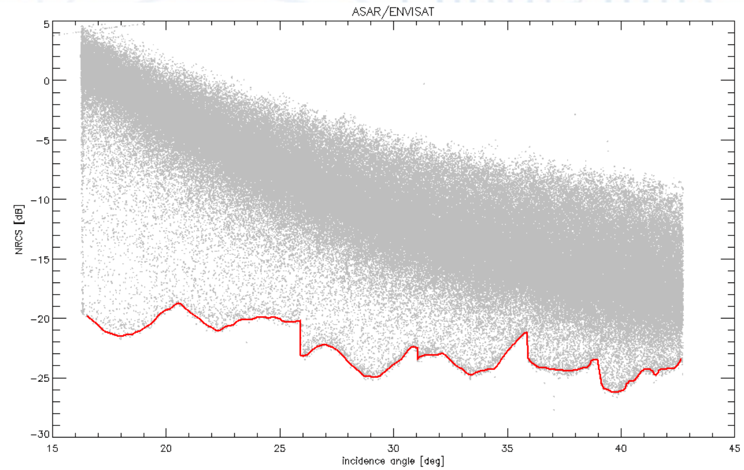

- NESZ is estimated for both VV and HH on a monthly basis
- Azimuth modulation is estimated for :
  - All bins of incidence angles : from 17 to 16°
    incidence bin step is 0.5°
    incidence bin size is 1°
  - All bins of wind speeds :
    wind bin step is 1 m/s
    wind bin size is 1 m/s

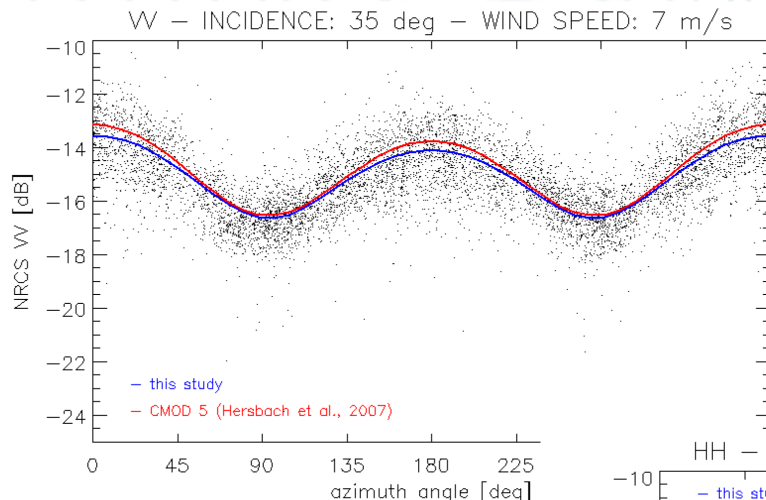

- Azimuth modulation is assumed to follow this relationship :

$$\sigma_0^{pp}(\theta,\phi,u_{10}) = a_0^{pp}(\theta,u_{10})[1 + a_1^{pp}(\theta,u_{10})\cos(\phi) + a_2^{pp}(\theta,u_{10})\cos(2\phi)]$$

- A Fit is done for all coefficients and available for users

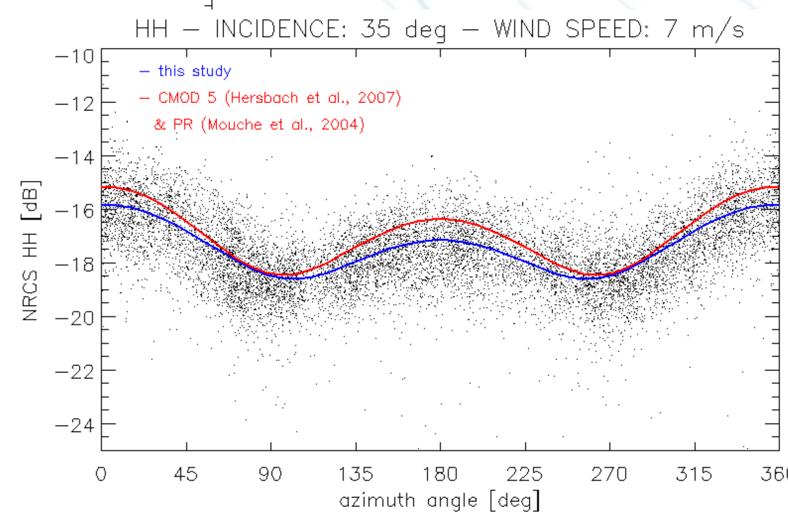

The Co-polarization Quest

- VV is found to be in line with CMOD-5 both for incidence angle dependency and azimuth modulation
- HH dependency is described for the first time directly from data.
- Reasonable agreement is found with previous methods based on CMOD+PR combination (less true for 15 m/s)

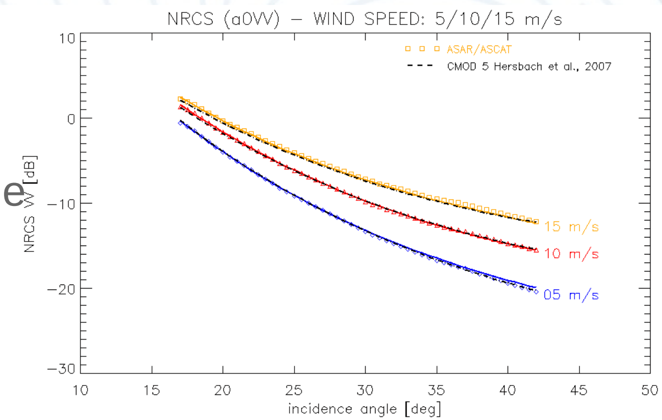

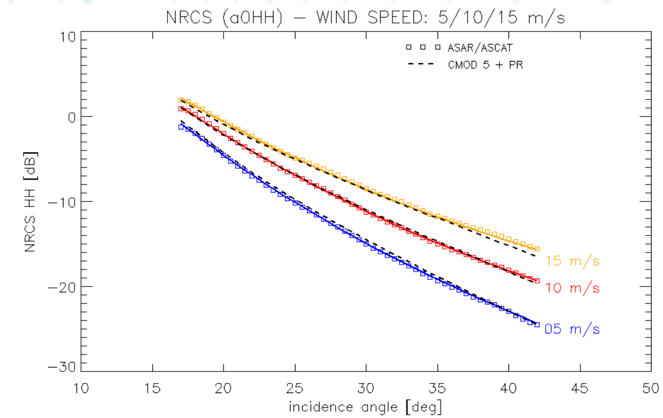

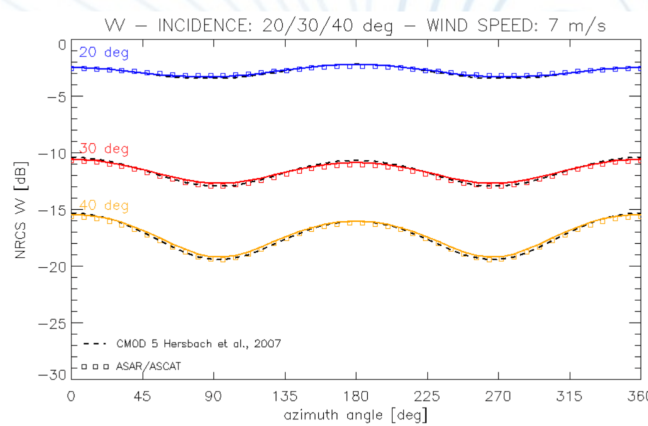

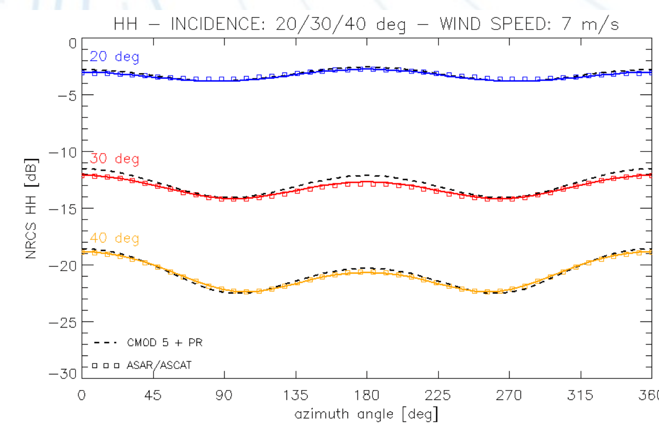

The Co-polarization Quest

- Polarization ratio deduced from this analysis unifies major findings from past litterature :
  - (i) The PR increases with increasing incidence angle, but at a signicantly lower level than standard 2-scale theories
  - (ii) The PR decreases with increasing wind speeds, in line with the results obtained using RS-2 data (e.g., [Zhang et al., 2011]) or model (e.g. [Kudryavtsev et al., 2003; Mouche et al., 2007]).
  - (iii) The azimuth modulation, as observed with airborne data [Mouche et al., 2005], in line with model development (e.g. [Kudryavtsev et al., 2003; Mouche et al., 2007b]), reaching maximum value in downwind.

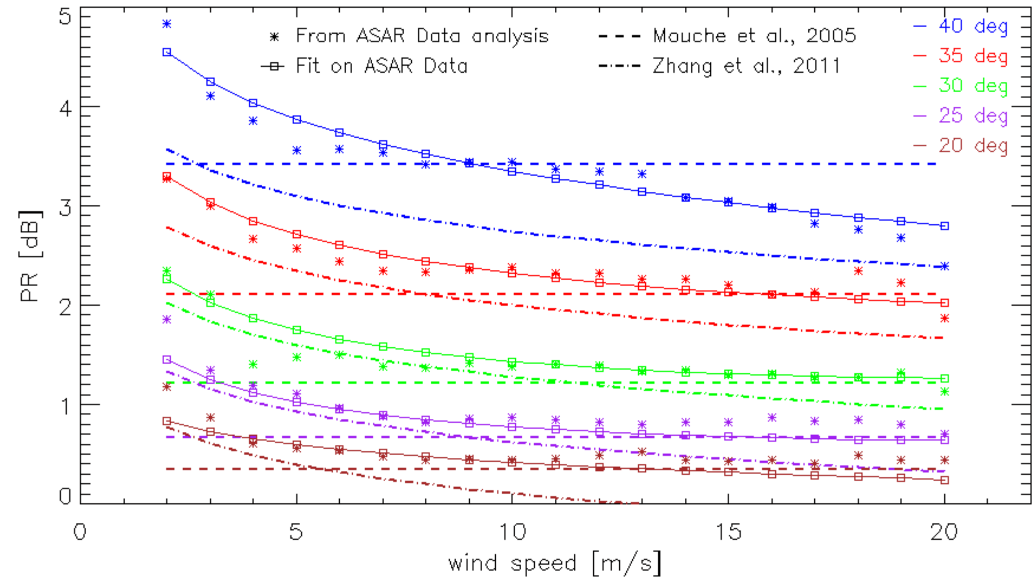

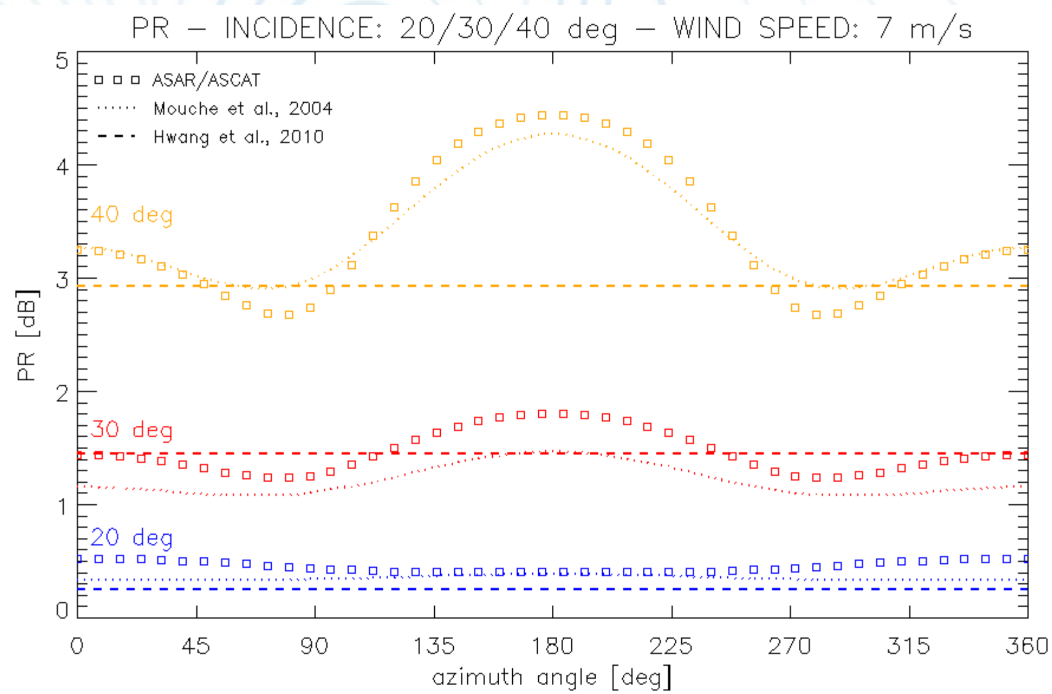

The Co-polarization Quest

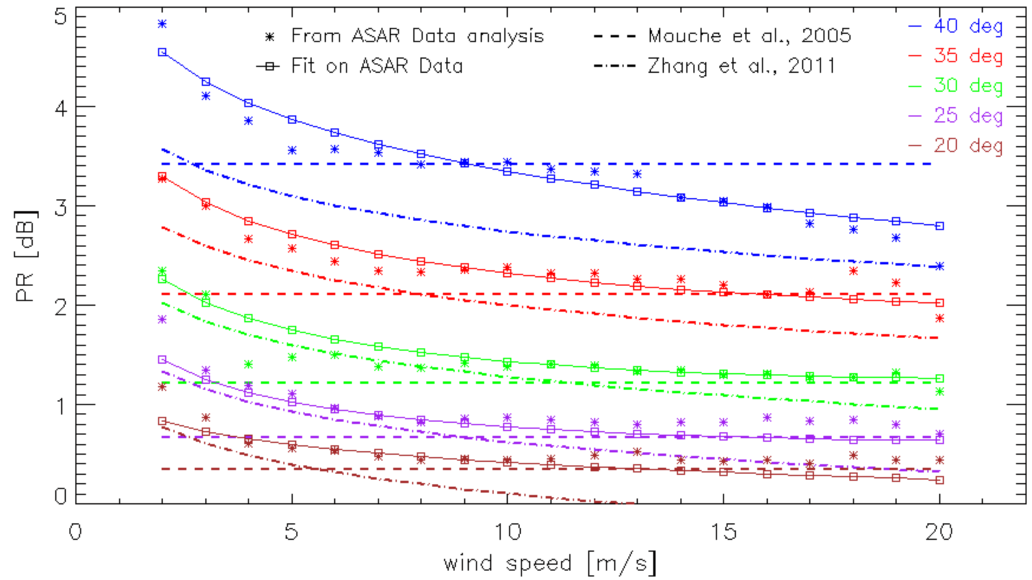

- The noise has to taken into account properly.

  Its relative importance compare to the sea backscatter increases when :
  - Incidence angles increase
  - Wind speeds decrease

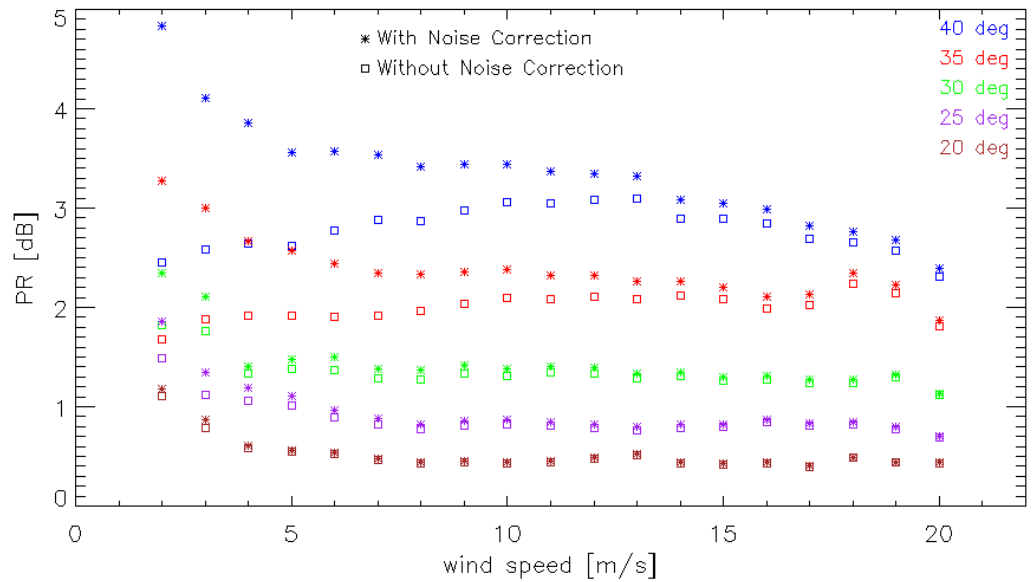

The Cross-polarization Odissey

- The signal is expected to be much lower than for co-polarization. Noise will be the main limitation
- NESZ is measured over area of low backscatter (e.g. ocean under low wind speed) and compared with theoretical profiles (dashed line)
- Mission requirement is -22dB (- - -)
- NESZ is within the requirement and following very well the theoretical profile if not better than it

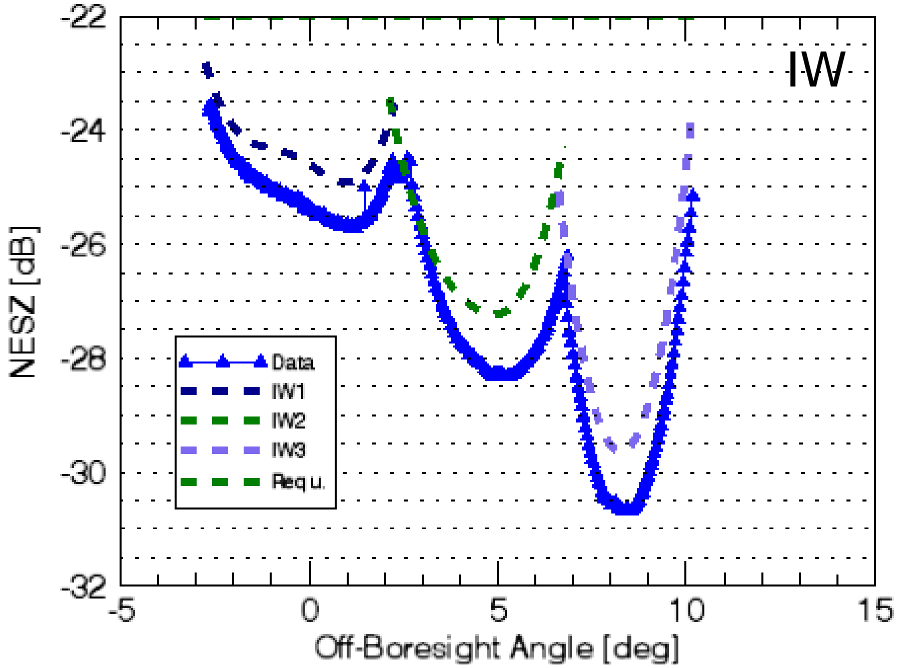

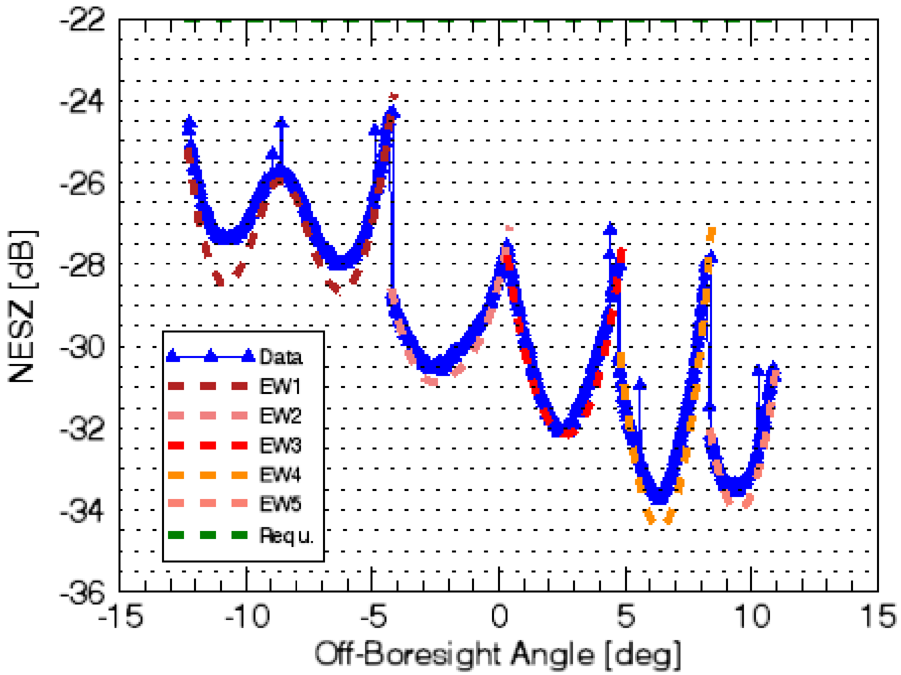

The Cross-polarization Odissey

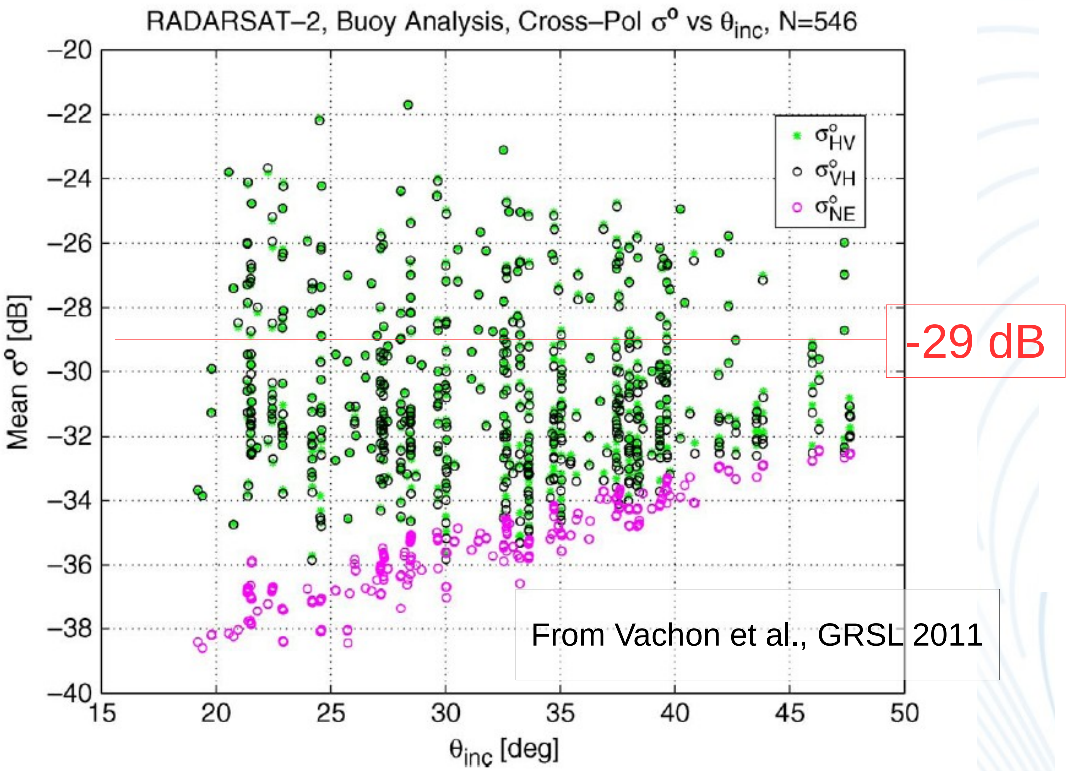

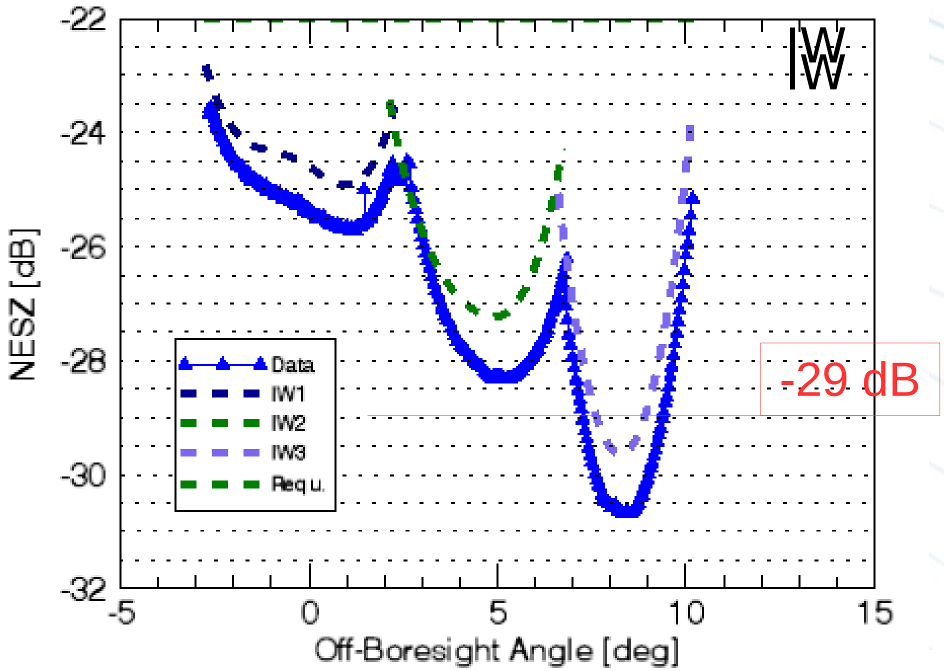

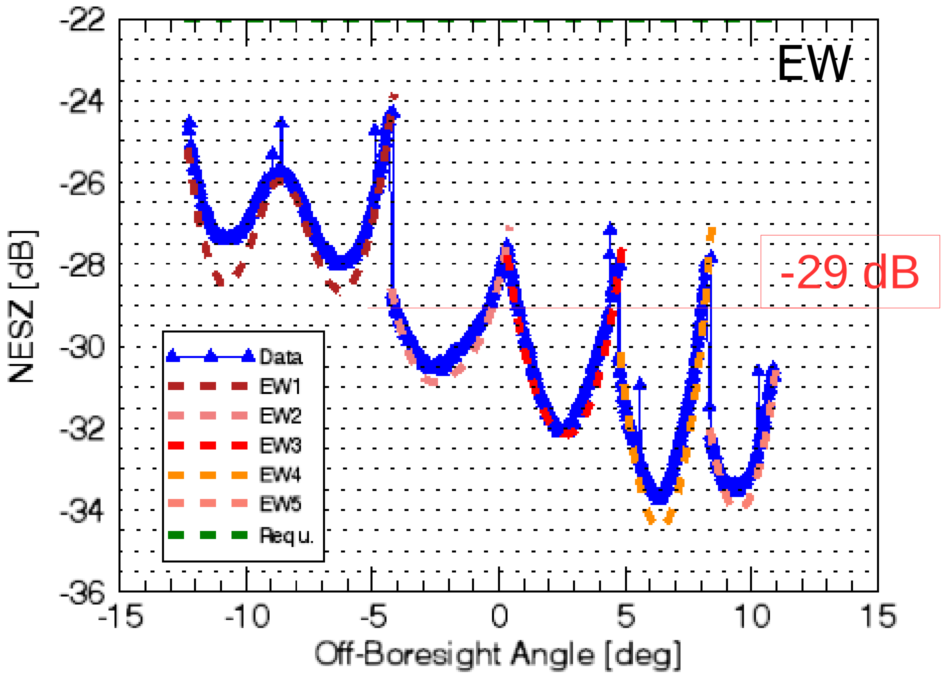

For Sentinel-1 A,
NESZ < -29 dB for largest incidences

EW Mode is close to RS-2 Quad-Pol NESZ for largest incidence angles

➡ Low values of NESZ for Sentinel-1 seems suitable for preparing VH GMF

Preliminary CP NRCS Analysis

- All Sentinel-1 A data acquired in cross-polarization have been processed up to Level-1 FR GRD by ESA PDGS using Terrain Observation with Progressive Scans SAR (TOPSAR).
- EW swath is 400 km wide and covers incidence angles from 19 to 47 degrees.

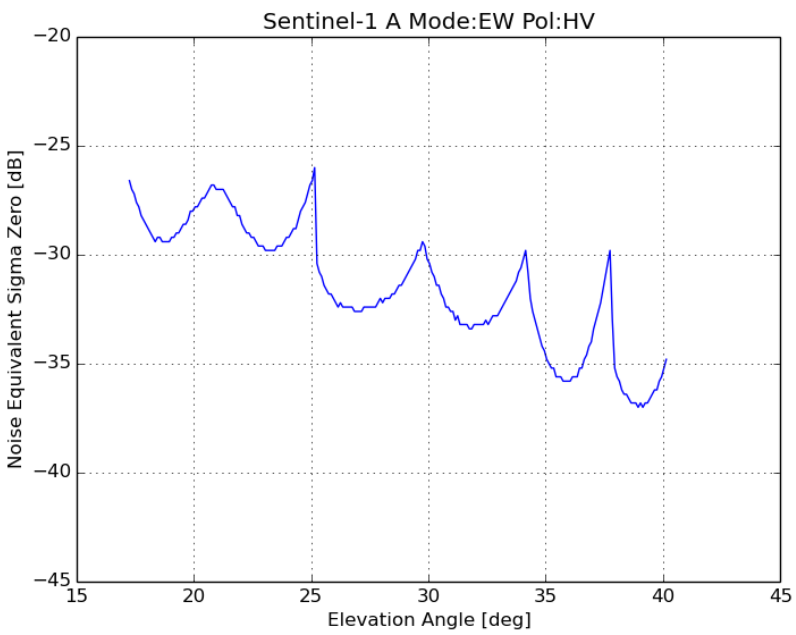

- NESZ is derived from the data set.
- NRCS are corrected from the NESZ.

Preliminary CP NRCS Analysis

- All Sentinel-1 A data acquired in cross-polarization have been processed up to Level-1 FR GRD by ESA PDGS using Terrain Observation with Progressive Scans SAR (TOPSAR).
- EW swath is 400 km wide and covers incidence angles from 19 to 47 degrees.

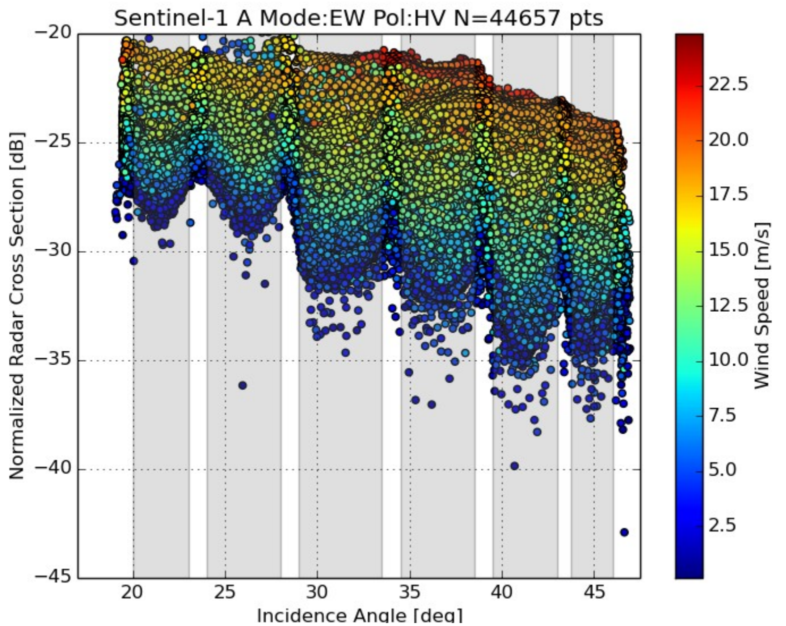

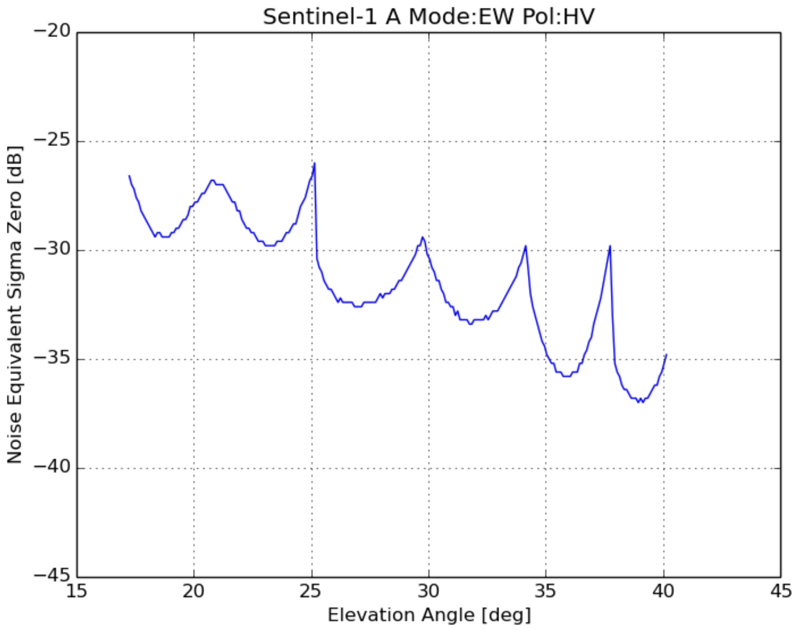

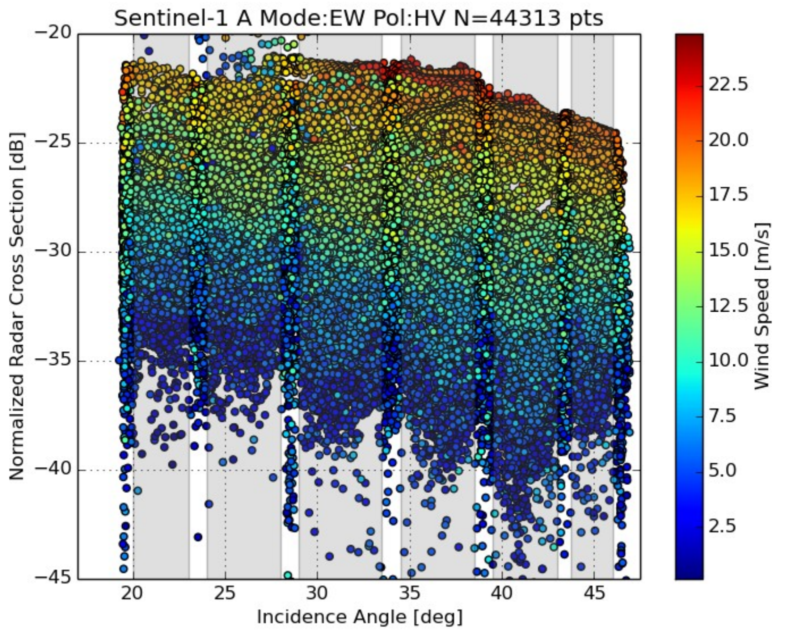

Preliminary CP NRCS Analysis

- All Sentinel-1 A data acquired in cross-polarization have been processed up to Level-1 FR GRD by ESA PDGS using Terrain Observation with Progressive Scans SAR (TOPSAR).
- EW swath is 400 km wide and covers incidence angles from 19 to 47 degrees.
- NESZ correction significantly impacts the results
- Dependence of NRCS with wind speed is observed from 2 to 22 m/s
- Dependence of NRCS with incidence angle is observed for this range of wind speeds

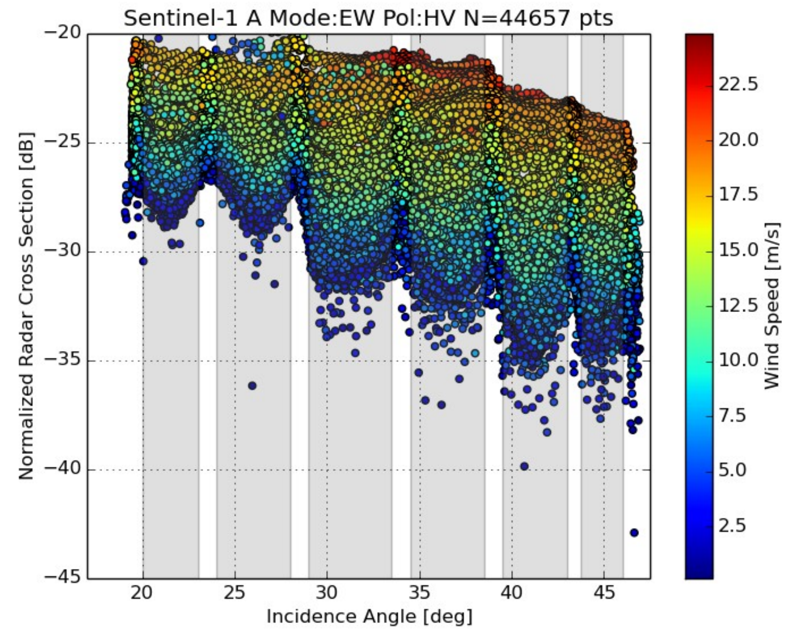

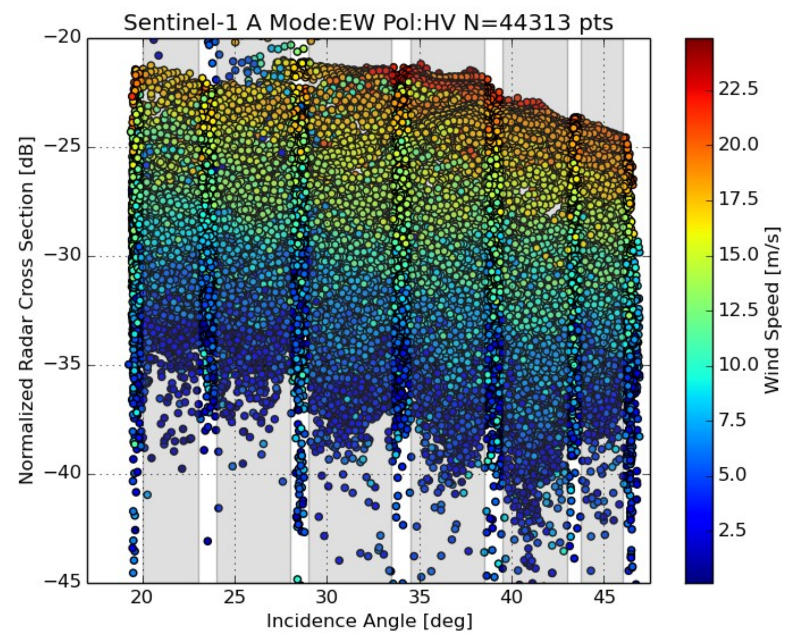

Preliminary CP NRCS Analysis

- All Sentinel-1 A data acquired in cross-polarization have been processed up to Level-1 FR GRD by ESA PDGS using Terrain Observation with Progressive Scans SAR (TOPSAR).
- EW swath is 400 km wide and covers incidence angles from 19 to 47 degrees.
- NESZ correction significantly impacts the results
- Dependence of NRCS with wind speed is observed from 2 to 22 m/s
- Dependence of NRCS with incidence angle is observed for this range of wind speeds. In line with last RS-2 study at 7 m/s

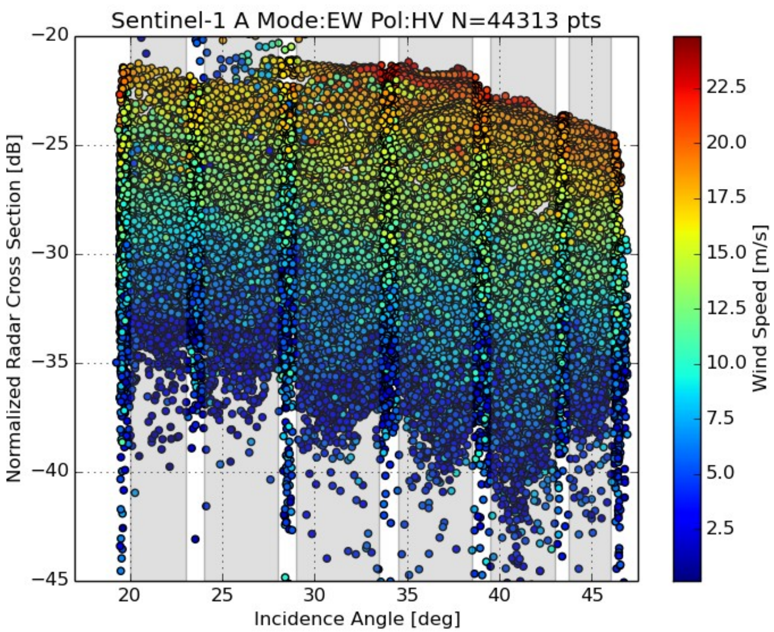

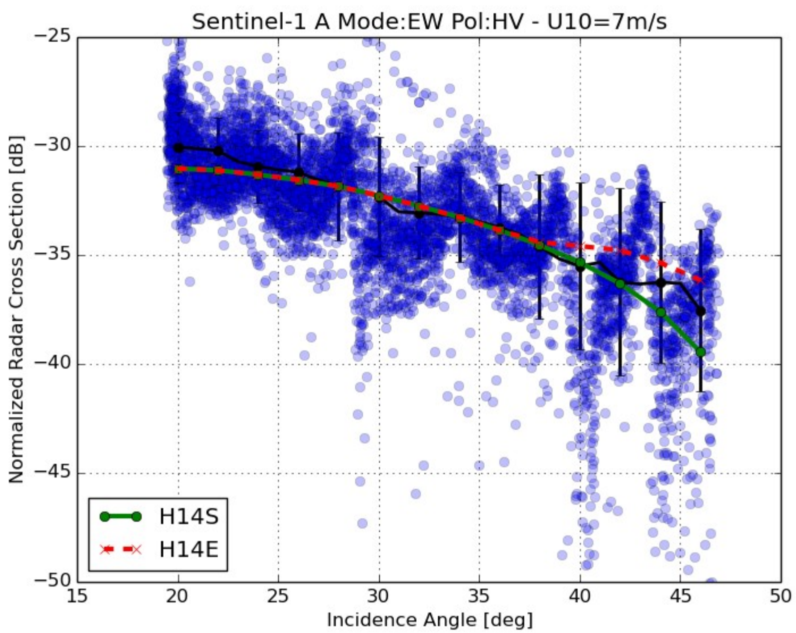

Preliminary CP NRCS Analysis

- Dependence of NRCS with wind speed has been observed for several incidence angles from light to medium wind speeds.
- Results are consistent with latest RS2 analysis from Hwang et al., 2014
- **To be continued…**

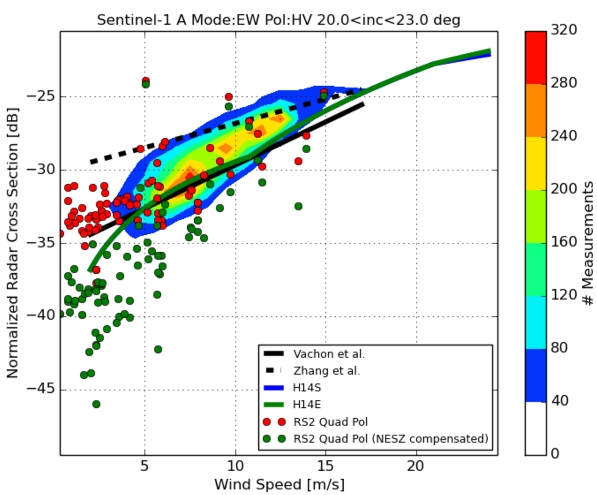

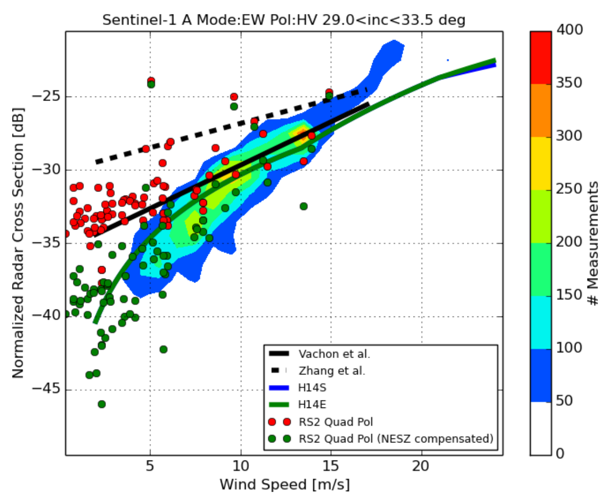

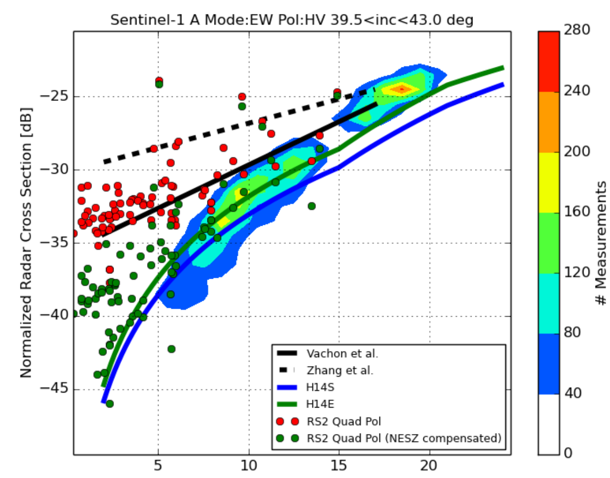

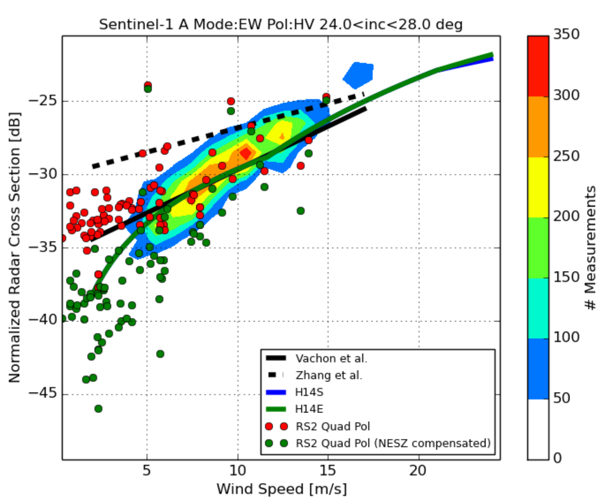

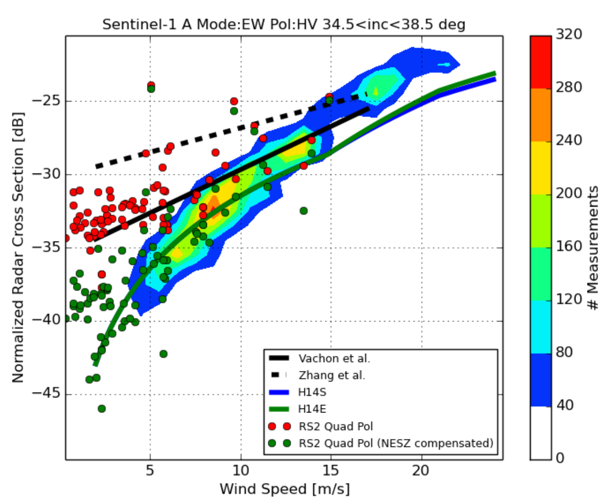

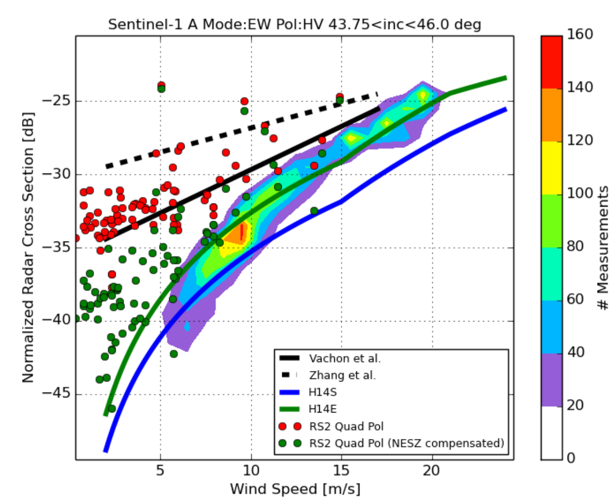

The Polarization combination : VV, HH & Azimuthal asymetries

$$\mathrm{UCA}^{pp}(\theta, U_{10}) = \frac{a_0^{pp} + a_2^{pp}}{a_0^{pp} - a_2^{pp}} - 1 \text{ [linear units]}$$

$$\mathrm{UCA}^{PD}(\theta, U_{10}) = \frac{(a_0^{vv} + a_2^{vv}) - (a_0^{hh} + a_2^{hh})}{(a_0^{vv} - a_2^{vv}) - (a_0^{hh} - a_2^{hh})} - 1 \text{ [linear units]}$$

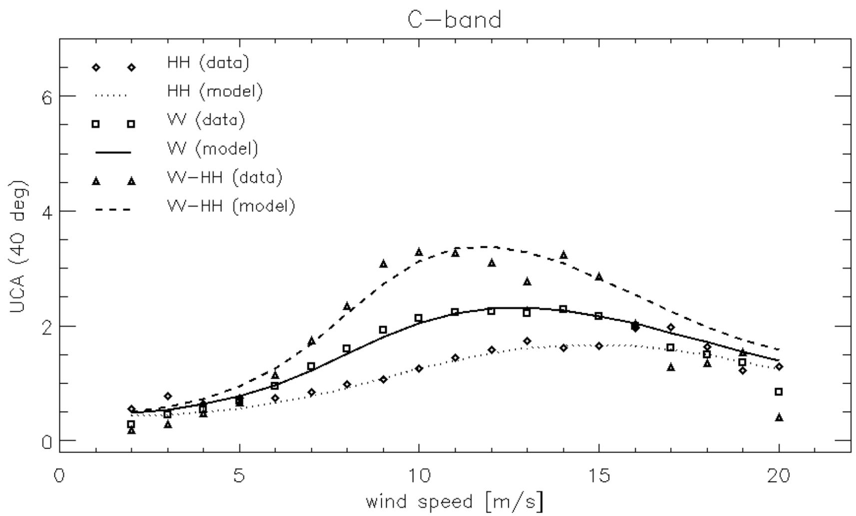

UCA for PD > UCA for VV > UCA for HH

- The NP part of the NRCS is more isotropic (UCA) than the polarizated part
- HH is more affected by the NP than VV.
- After 12 m/s the sensitivity of the signal in Crosswind to the wind seems to less saturate than in Upwind

$$\mathrm{UDA}^{pp}(\theta, U_{10}) = \frac{a_1^{pp}}{a_0^{pp}} \text{ [linear units]}$$

$$\mathrm{UDA}^{PD}(\theta, U_{10}) = \frac{a_1^{vv} - a_1^{hh}}{a_0^{vv} - a_0^{hh}} \text{ [linear units]}$$

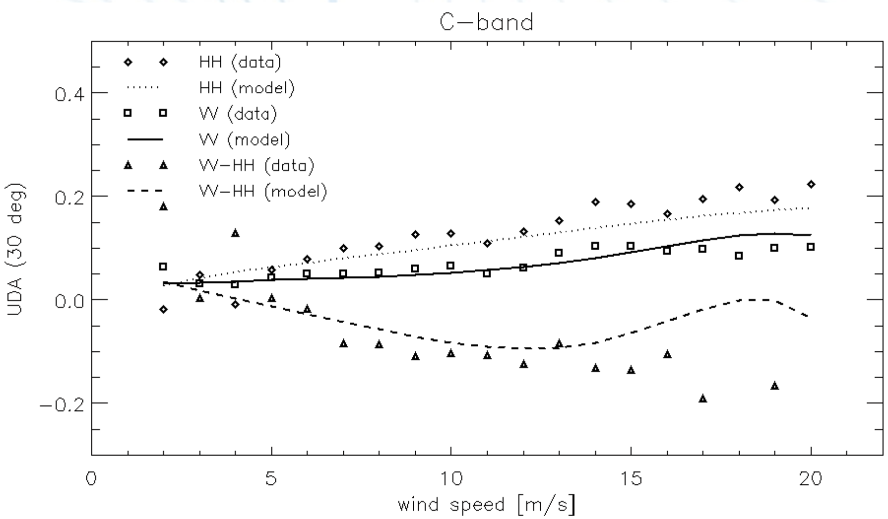

UDA for PD <0. UDA for VV < UDA for HH

- The UDA observed in VV and HH is not coming from Bragg waves through 2 scale-Bragg model
- NP is strongly anisotropic between upwind and downwind configuration
- Relative importance of Bragg waves is more pronounced in Downwind than in Upwind

The Polarization combination : VV, HH & Azimuthal asymetries

- PR and PD are larger for downwind observations compared to upwind ones.

➔ This indicates a more predominant impact of non-resonant scatters for upwind conditions.

It helps interpretring Doppler analysis

$$\bar{c} = \int c(\vec{k})\Lambda(\vec{k})\mathrm{d}\vec{k} / \int \Lambda(\vec{k})\mathrm{d}\vec{k}$$, where

$\Lambda(\vec{k})d\vec{k}$ represents the relative contribution to the total radar cross section related to wave number in the range $\vec{k}$ to $\vec{k} + d\vec{k}$

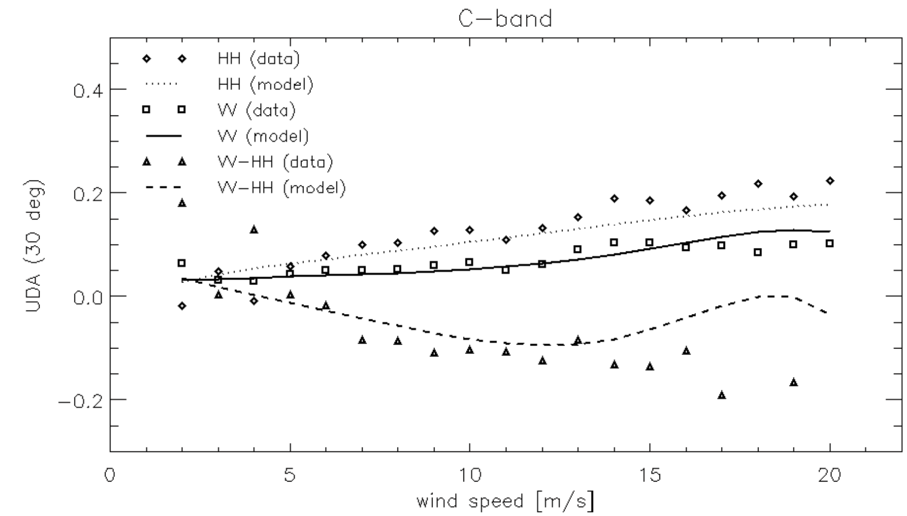

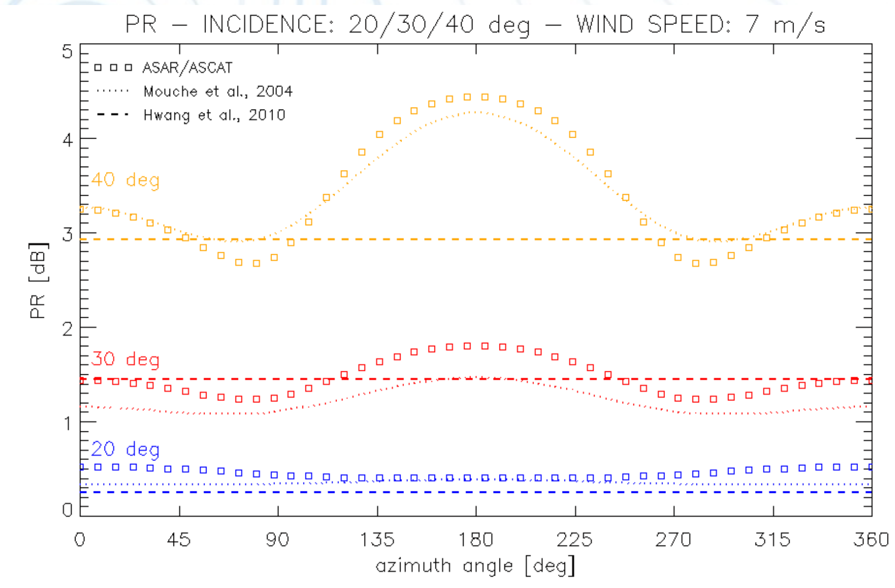

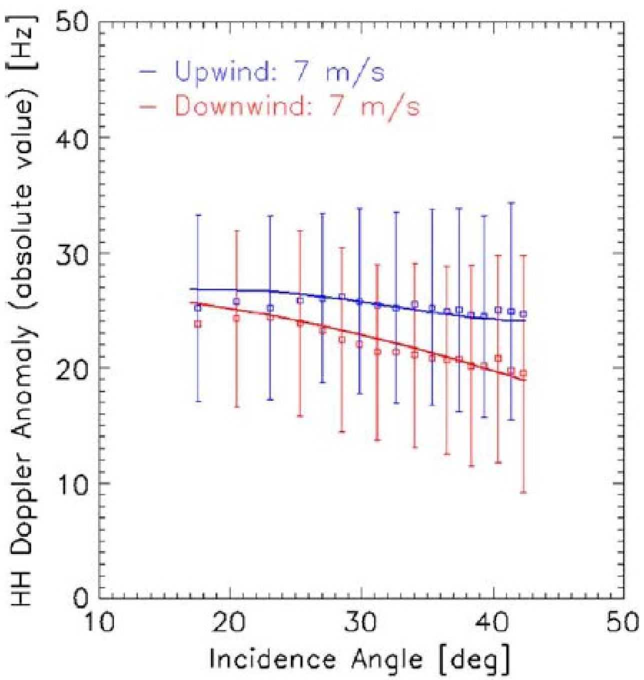

The Polarization combination : Co and Cross polarization

- Close co-variations between CP and PD under light to moderate wind conditions.
- Beyond 8-9 m/s, CP is then clearly found more responsive to wind speed change than PD.
-

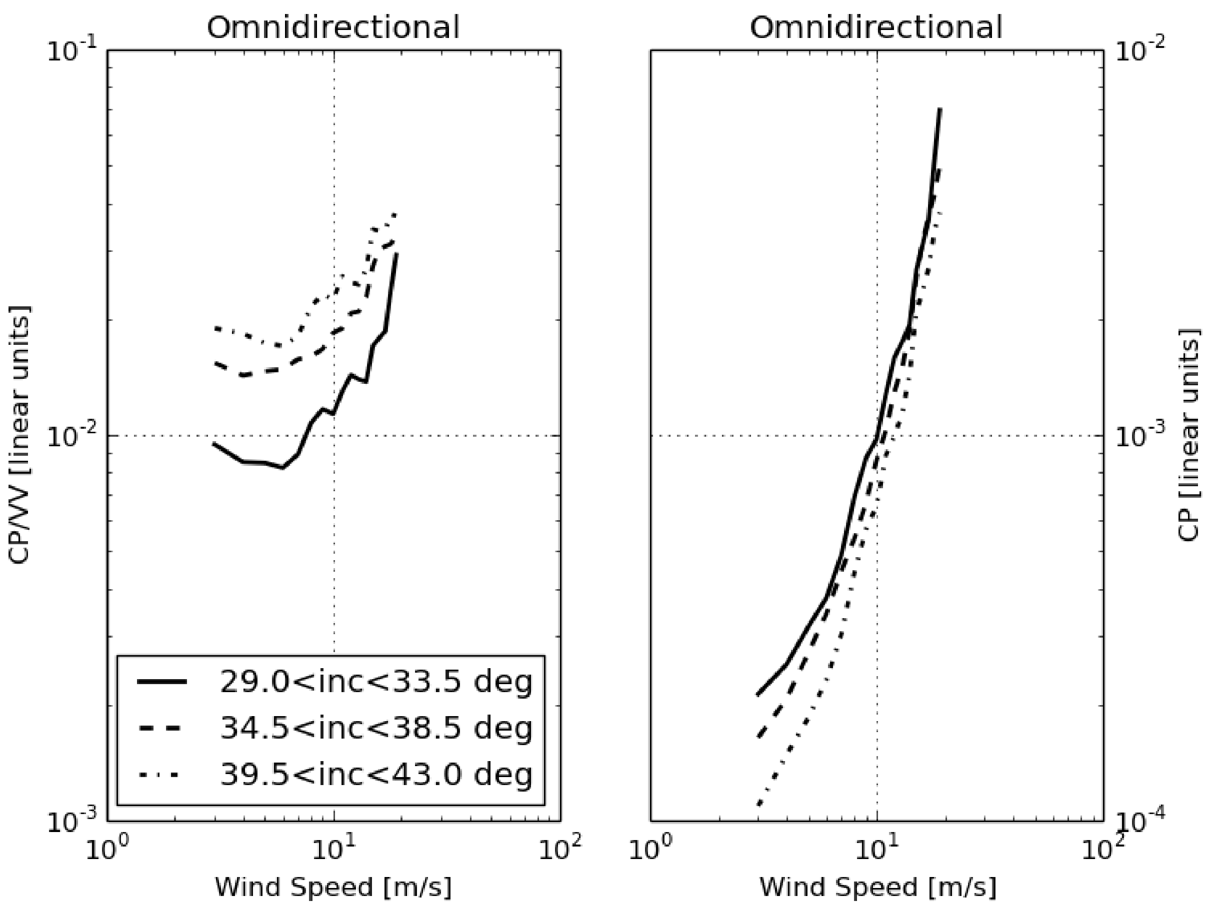

The Polarization combination : Co and Cross polarization

- Close co-variations between CP and PD under light to moderate wind conditions.
- Beyond 8-9 m/s, CP is then clearly found more responsive to wind speed change than PD.
- In line with UCA analysis, this threshold wind may well correspond to the onset of vigorous breaking events, large enough to directly impact C-band in- and out-of-plane local tilts.
- For particular cases, *Kudryavtsev et al. [2014]* reported very signicant CP/PD and PR variations over strong surface current gradient areas, to demonstrate and quantitatively evaluate the relative impact of breakers on CP and PR signals. Although the process causing wave breaking is different, this is consistent with the present analysis, with a clear departure of CP/PD within the high wind speed regime.

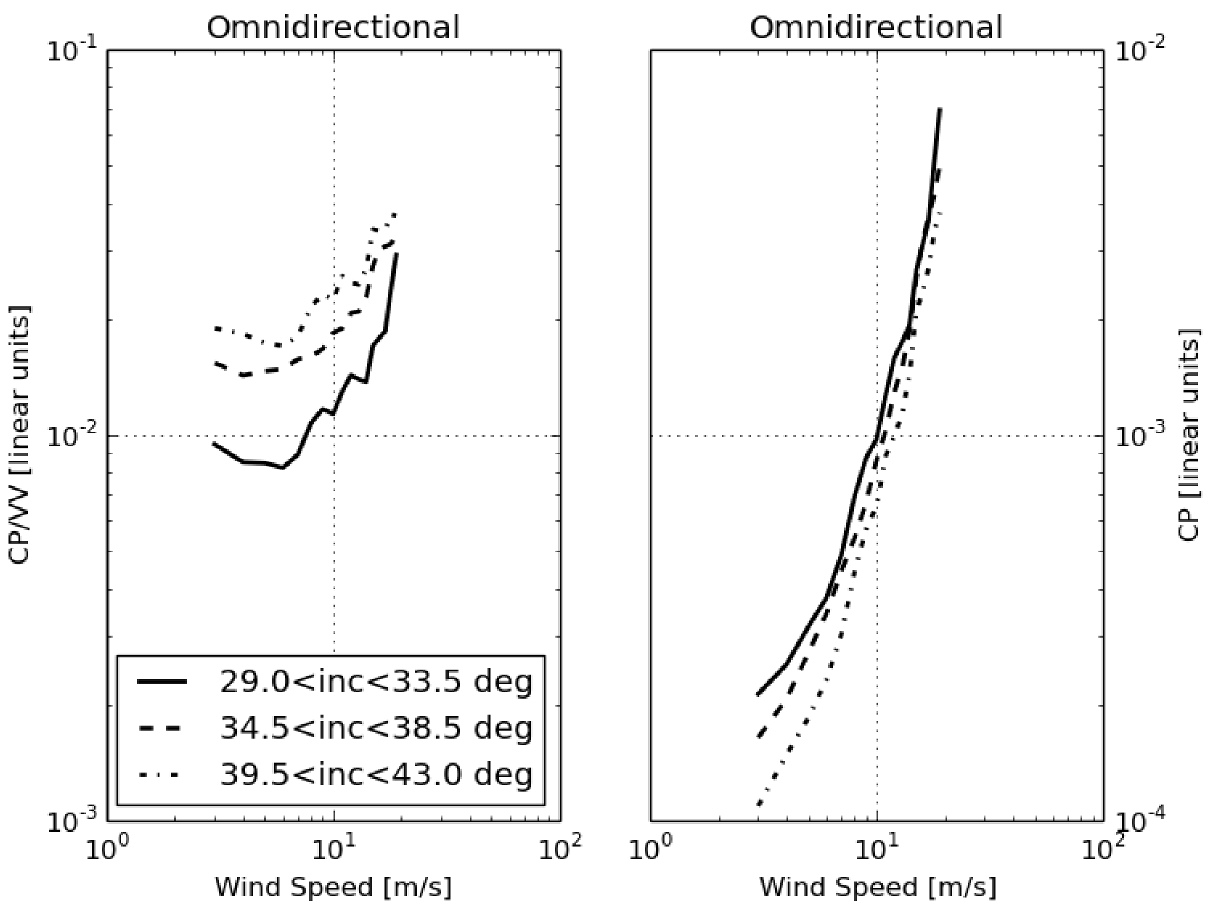

The Polarization combination : Co and Cross polarization

- In line with UCA analysis, this threshold wind may well correspond to the onset of vigorous breaking events, large enough to directly impact C-band in- and out-of-plane local tilts.

- Considering that HH polarization best minimizes the polarized resonant contribution, especially for cross-wind conditions, it can thus be anticipated that both HH NRCS for cross-wind and CP shall exhibit comparable wind speed relationship, through a comparable sensitivity to breaking occurrence.

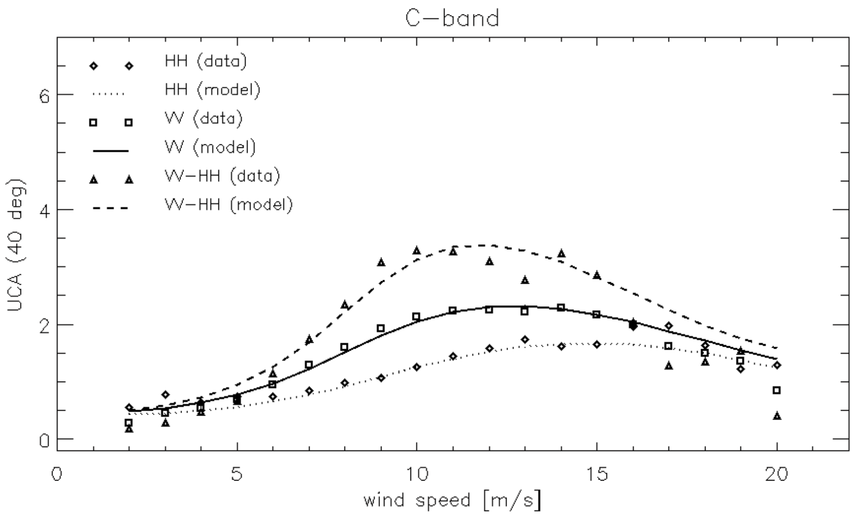

The Polarization combination : Co and Cross polarization

- In line with UCA analysis, this threshold wind may well correspond to the onset of vigorous breaking events, large enough to directly impact C-band in- and out-of-plane local tilts.

- Considering that HH polarization best minimizes the polarized resonant contribution, especially for cross-wind conditions, it can thus be heuristically anticipated that both HH NRCS for cross-wind and CP shall exhibit comparable wind speed relationship, through a comparable sensitivity to breaking occurrence.

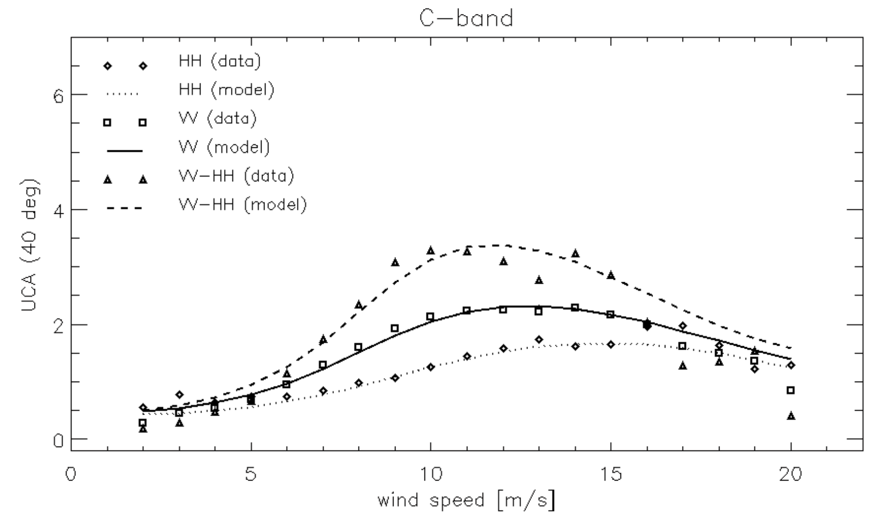

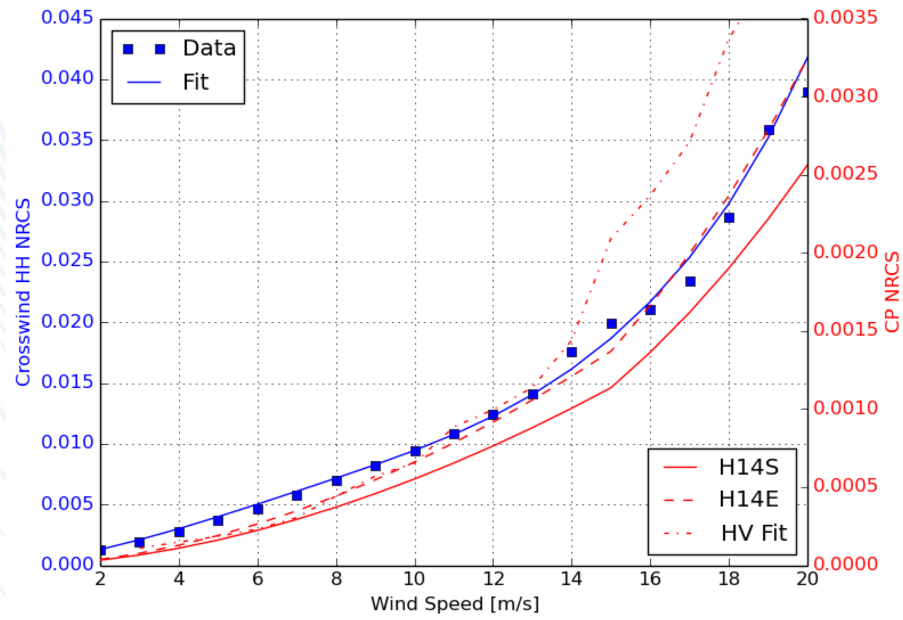

NRCS, Doppler & Downdraft

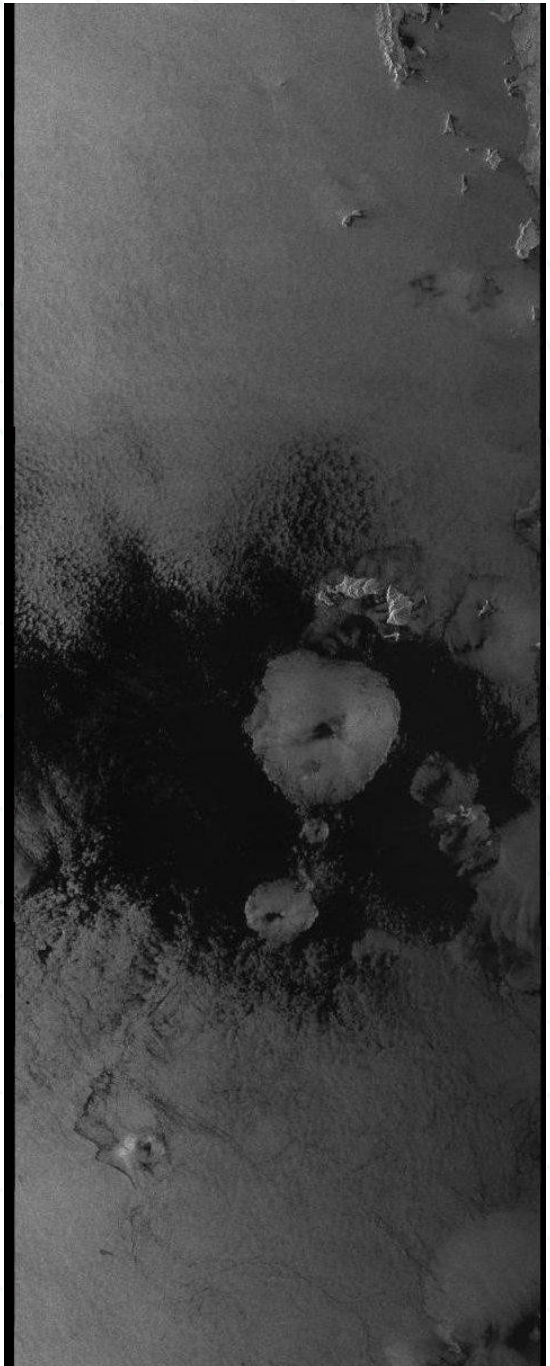

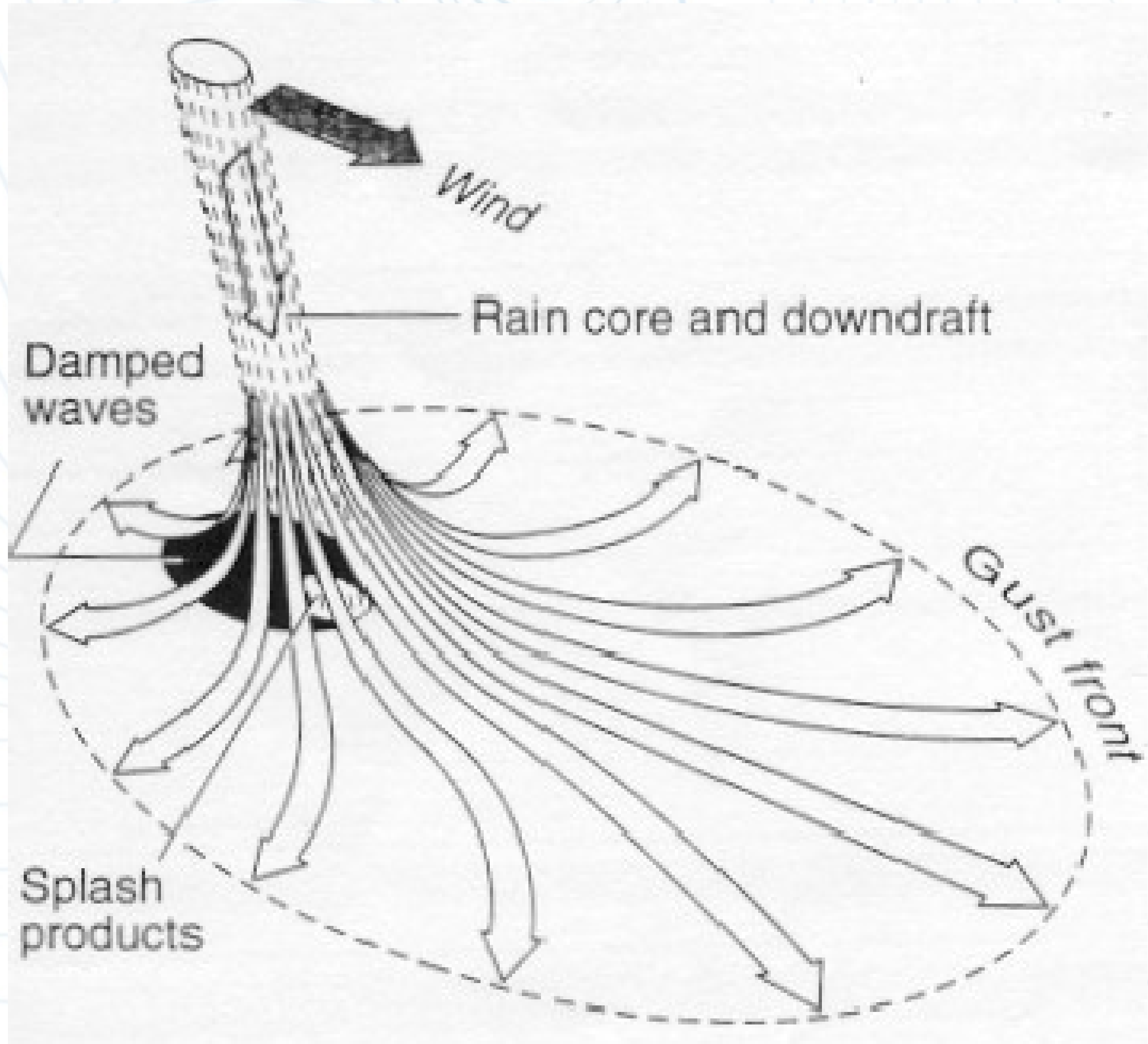

Schematic sketch of the **downdraft of a rain cell,** spreading over the sea surface and causing roughening of the sea surface; (adapted from Atlas, 1994b).

NRCS, Doppler & Downdraft

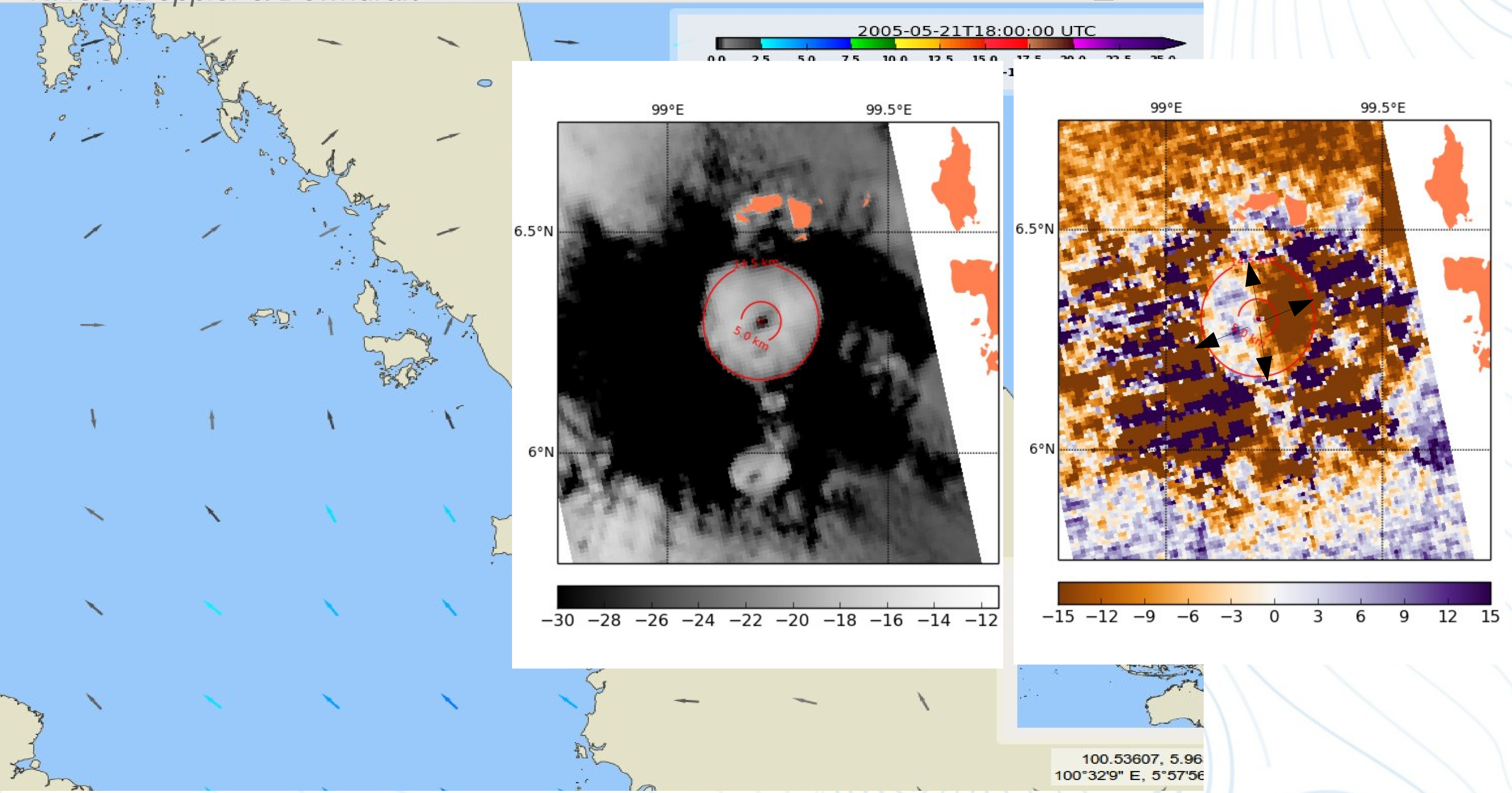

Outside the rain cells, Doppler variation is consistent with model wind
Inside the rain cells, Doppler sign is consistent with downdraft shape (with circular gust front)

NRCS, Doppler & Downdraft

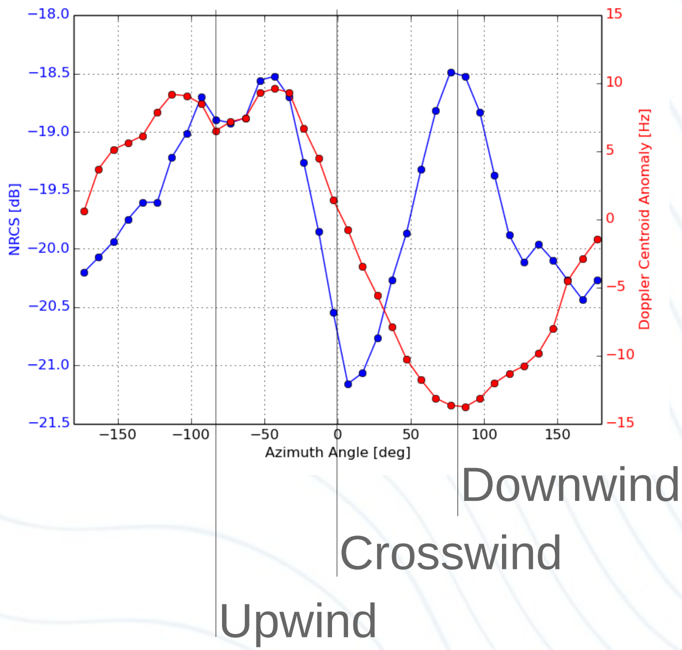

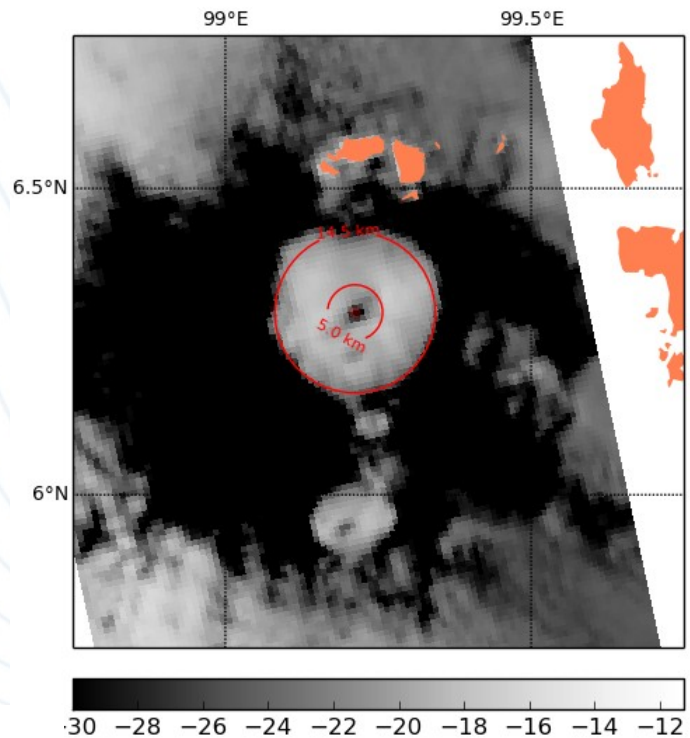

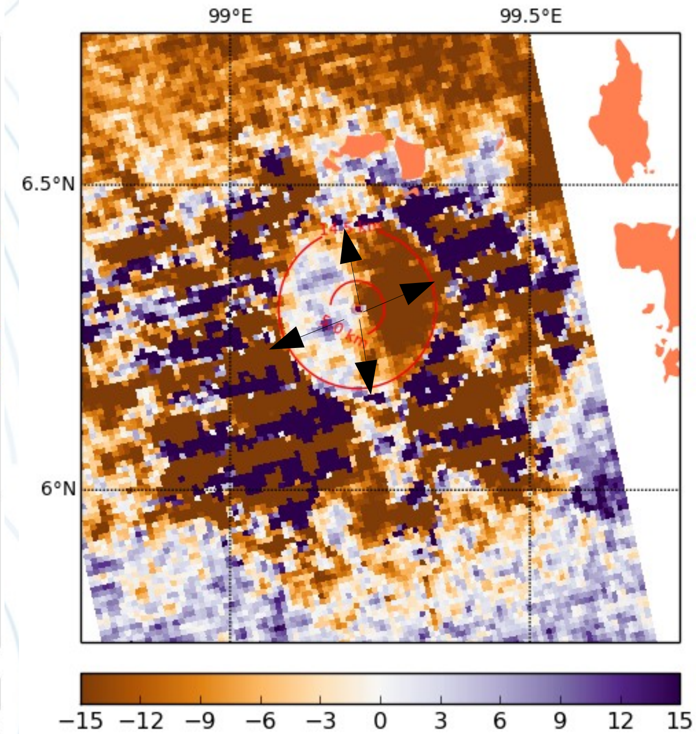

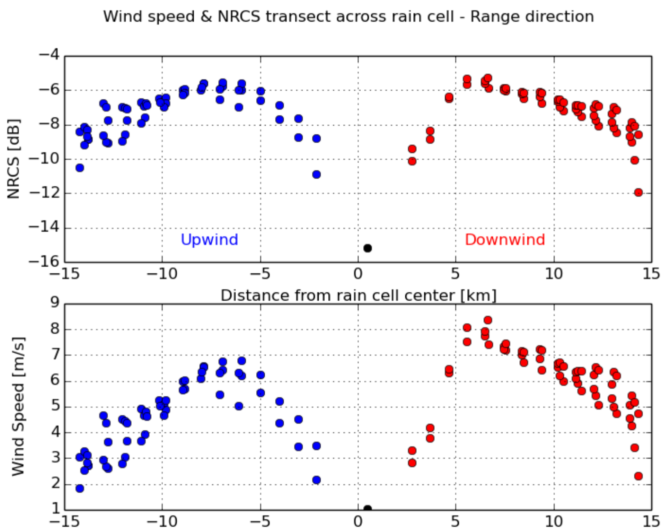

- Inside the rain cells, Doppler & NRCS variation are consistent
- CMOD-like model are certainly not applicable (short fetch). Do we see waves development from the center of the cell to the gut front ?
- Vertical motion may be retrieved from cell size, shape and NRCS gradient ?

NRCS, Doppler & Downdraft

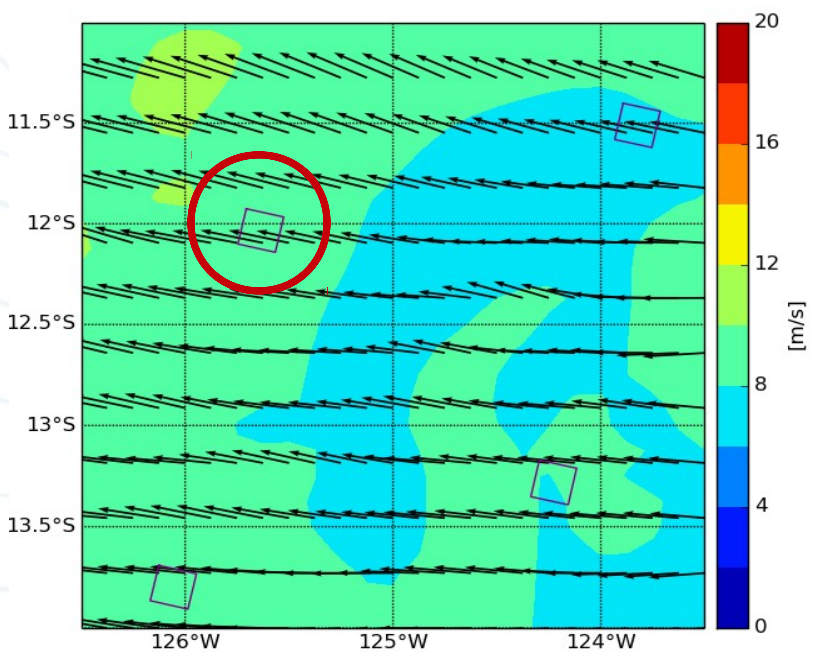

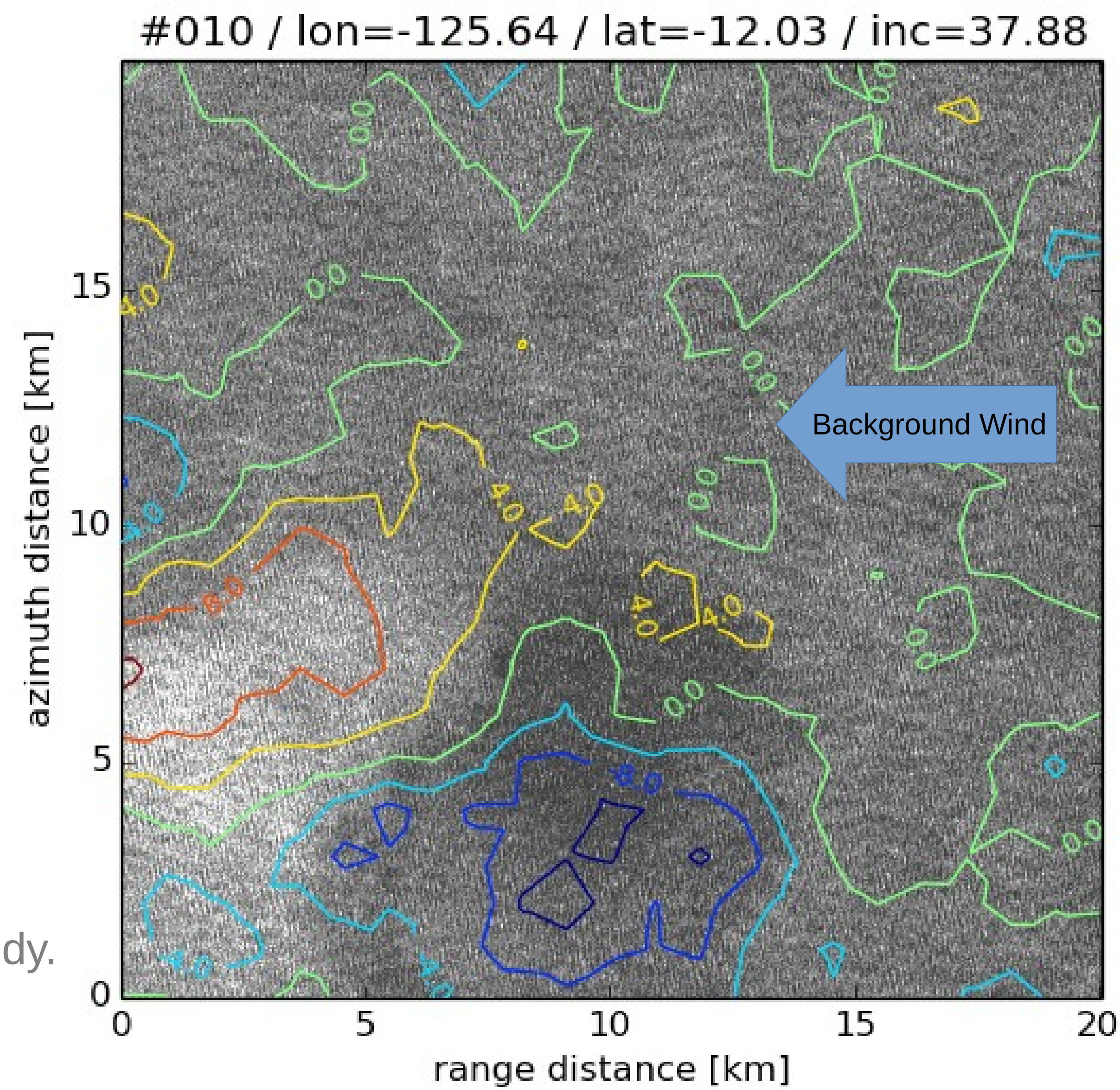

- Imagette #10 is considered for this study.
- Incidence angle is 37.88 degrees
- Polarization is HH
- Wind is blowing in range direction

NRCS, Doppler & Downdraft

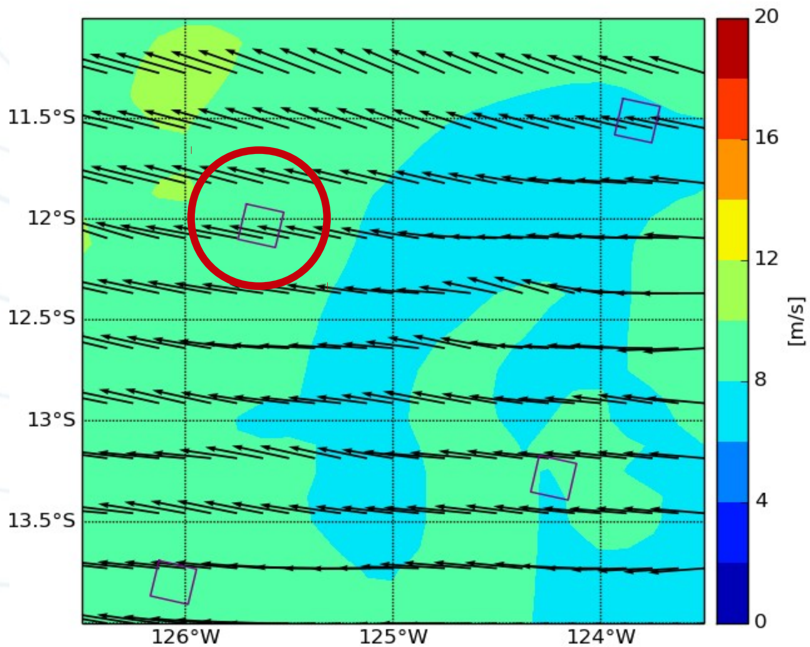

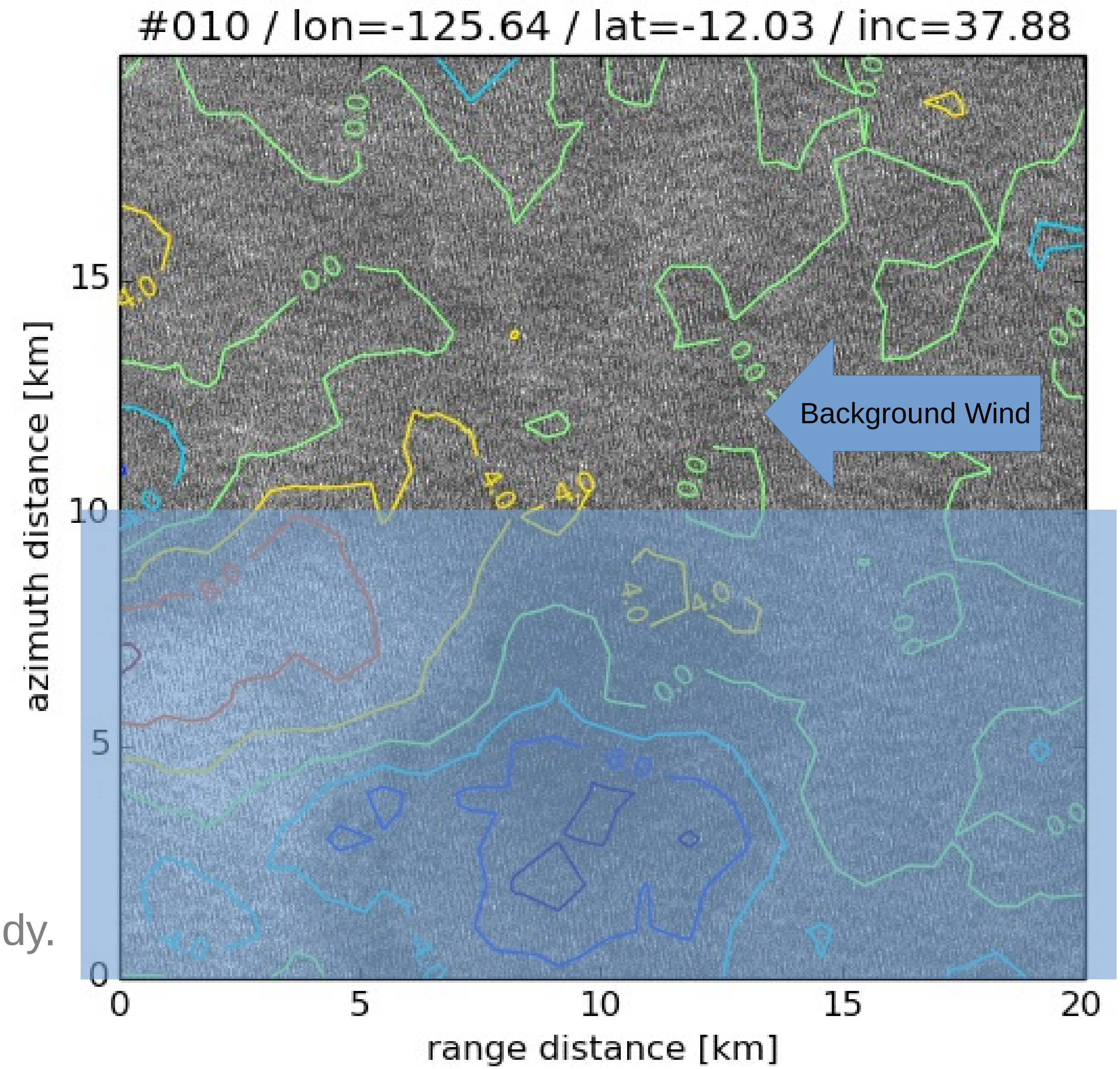

- Imagette #10 is considered for this study.
- Incidence angle is 37.88 degrees
- Polarization is HH
- Wind is blowing in range direction

NRCS, Doppler & Downdraft

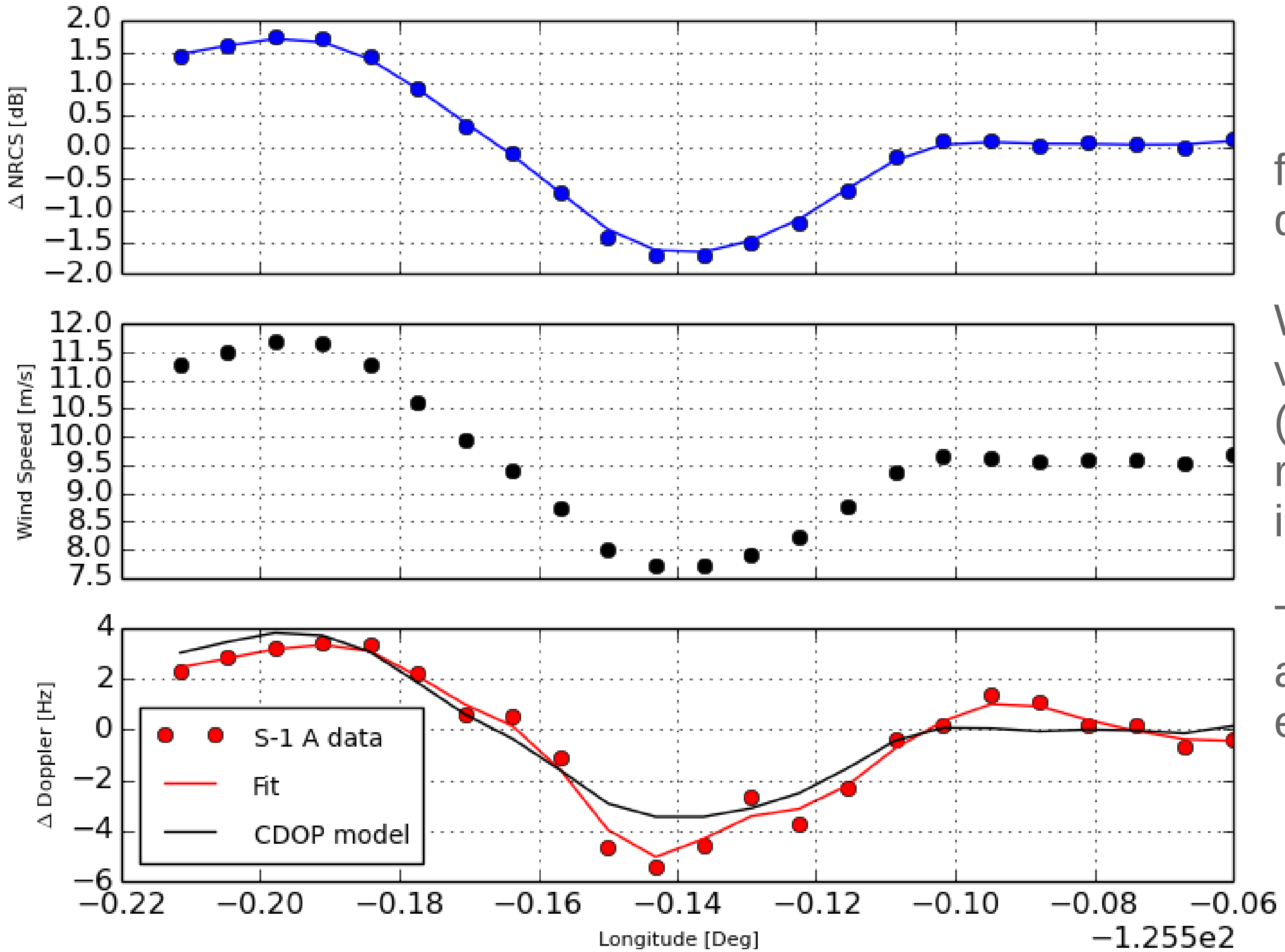

wind speed variations retrieved from NRCS for a constant wind direction according to CMOD-5.

When applying these wind speed values into our Doppler GMF (CDOP), we are able to reproduce the Doppler variation inside the rain cell.

This confirms that both NRCS and Doppler are affected by wind effect

Global Ku- and Ka- near nadir measurements

Elements for discussion & Focus on Sea-Ice

Context

2 CNES Missions with Ocean applications are planned

- SWOT (CNES/NASA, 2020)
  - Ka-Band KaRin

- CFOSAT (CNES/CNSA, 2018)
  - Ku-Band SWIM (waves scatterometer)
  - Ku-Band SCAT (wind scatterometer)

→ Ku and Ka-Band measurements from CNES missions will be available soon over ocean at low incidence angles, where not much as been done yet

GPM (JPL/JAXA) mission for precipitation has 2 radars in Ka and Ku Band operating at low incidence angles

Context

Ifremer is involved in the preparation of these 2 missions (for the ocean component) to :

- Improve our understanding of electromagnetic and oceanic waves (sea-ice) interactions at low incidence angles
- Develop ocean products
- Anticipate Science Applications
- Prepare the Cal/Val phase (for CFOSAT)

➡ GPM may be a good opportunity to get a flavor of what could be done at low incidence angles in Ku and Ka-Band

The GPM Mission: Instrument & Acquisition pattern

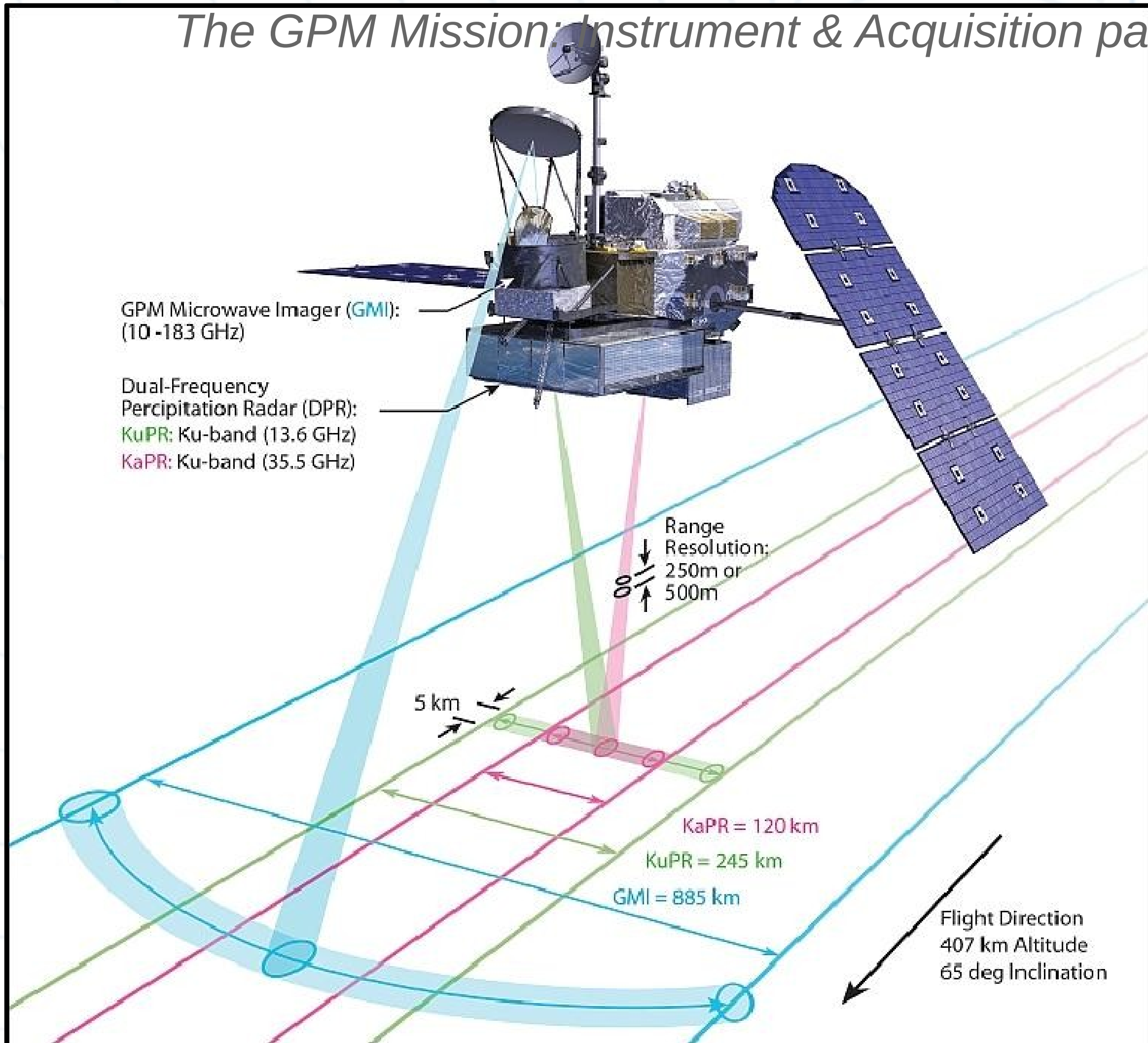

Quasi-simultaneaous observations are available from both KaPR and KuPR in the quasi-specular domain :
inc ϵ [-18,18] Ku PR
inc ϵ [-9, 9] Ka PR

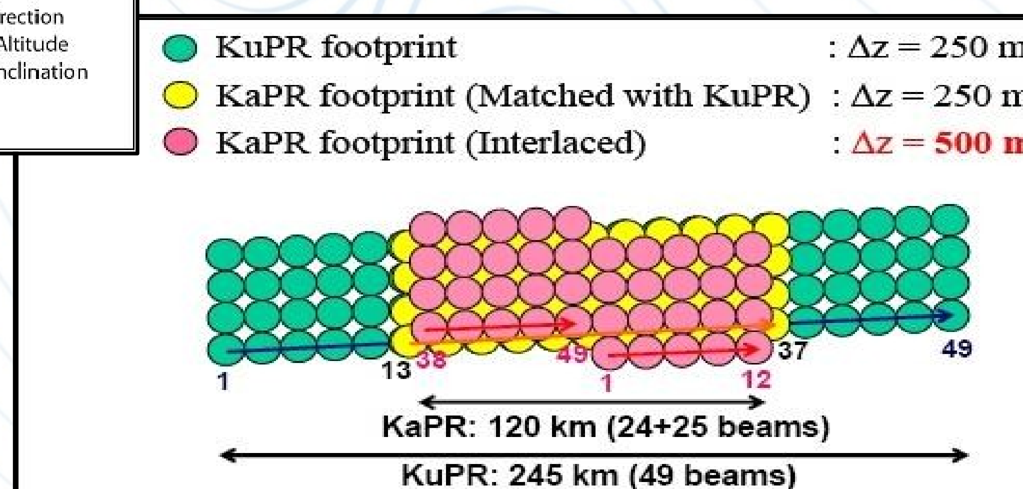

The GPM Mission: Instrument & Acquisition pattern

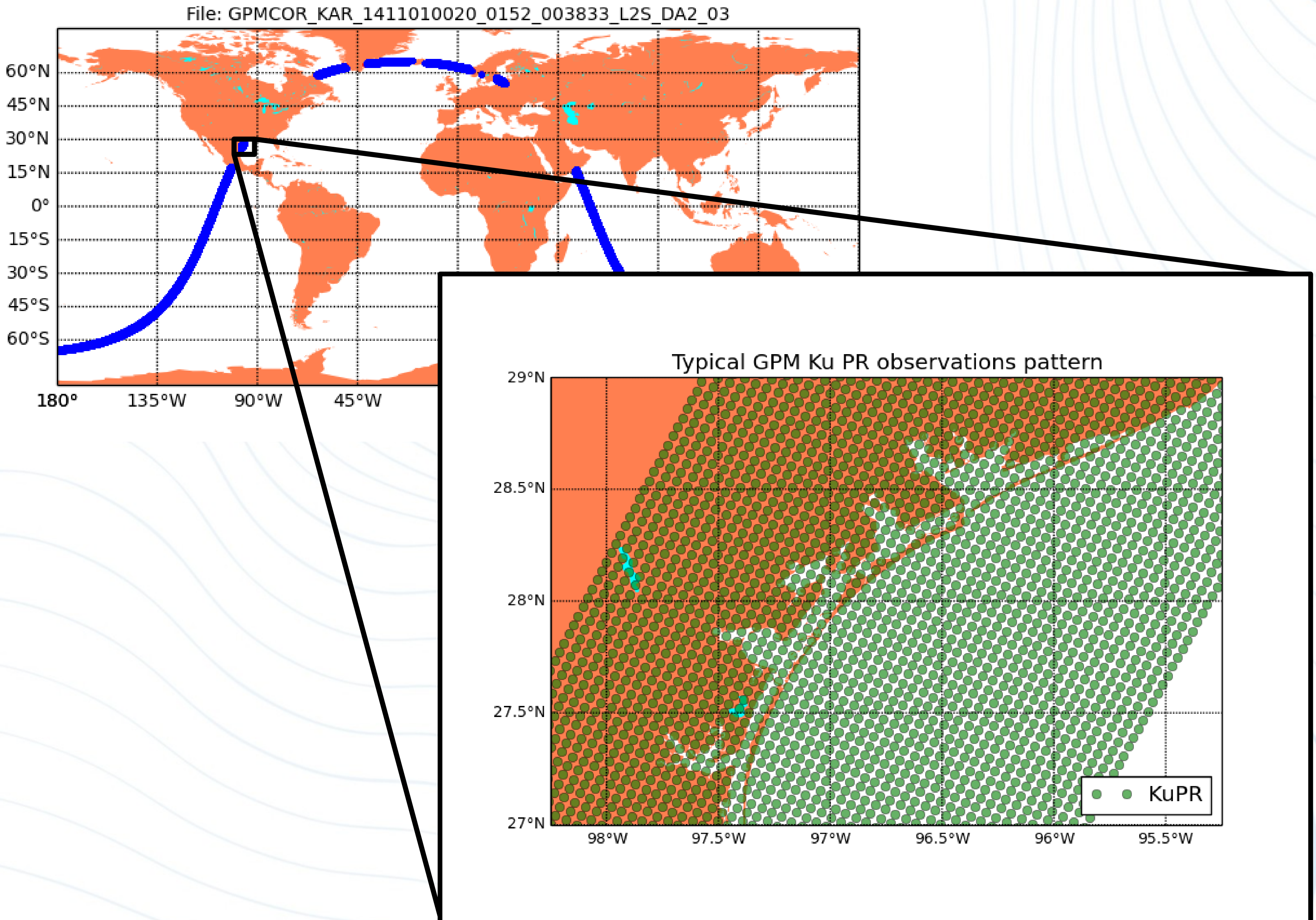

The GPM Mission: Instrument & Acquisition pattern

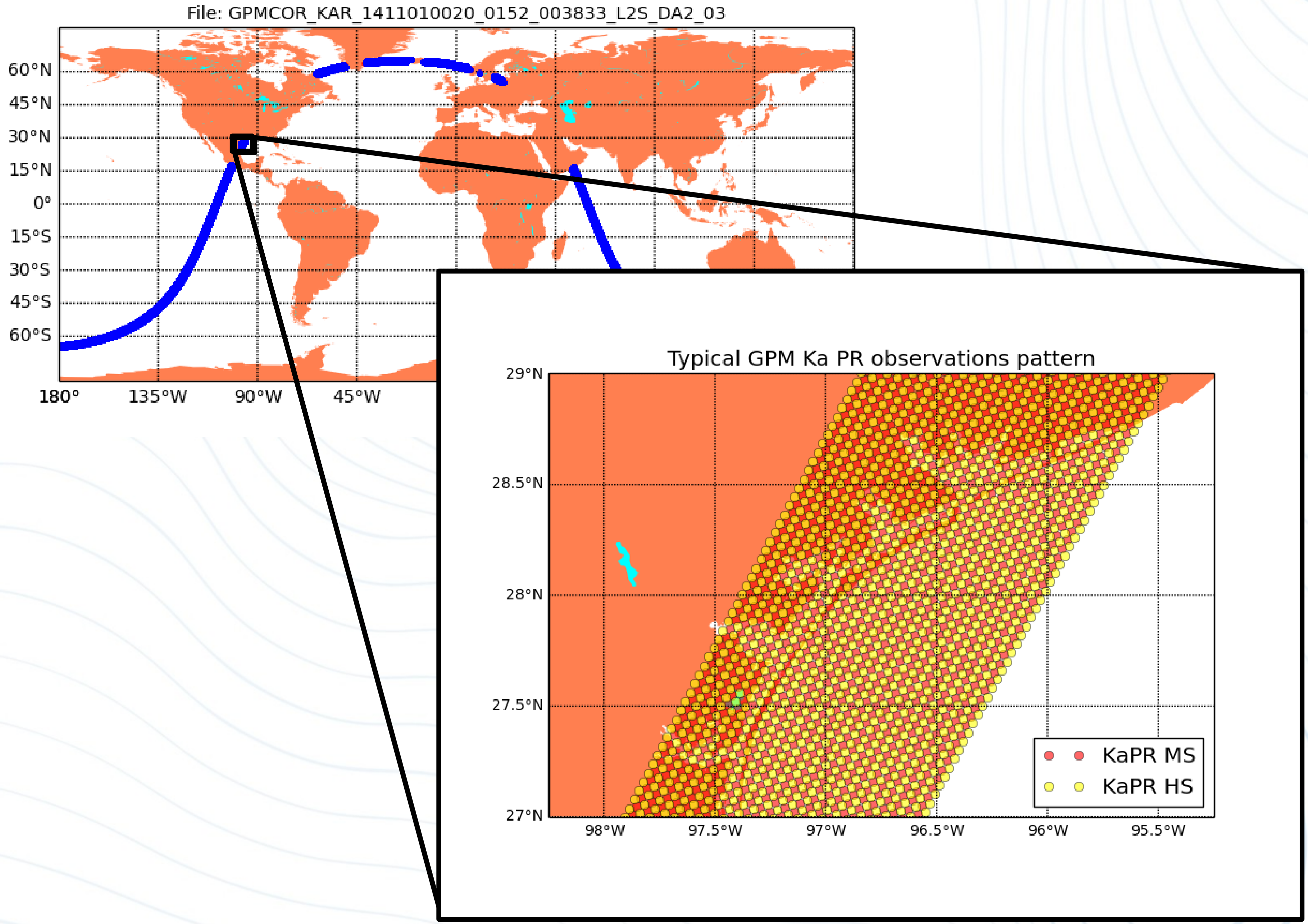

The GPM Mission: Instrument & Acquisition pattern

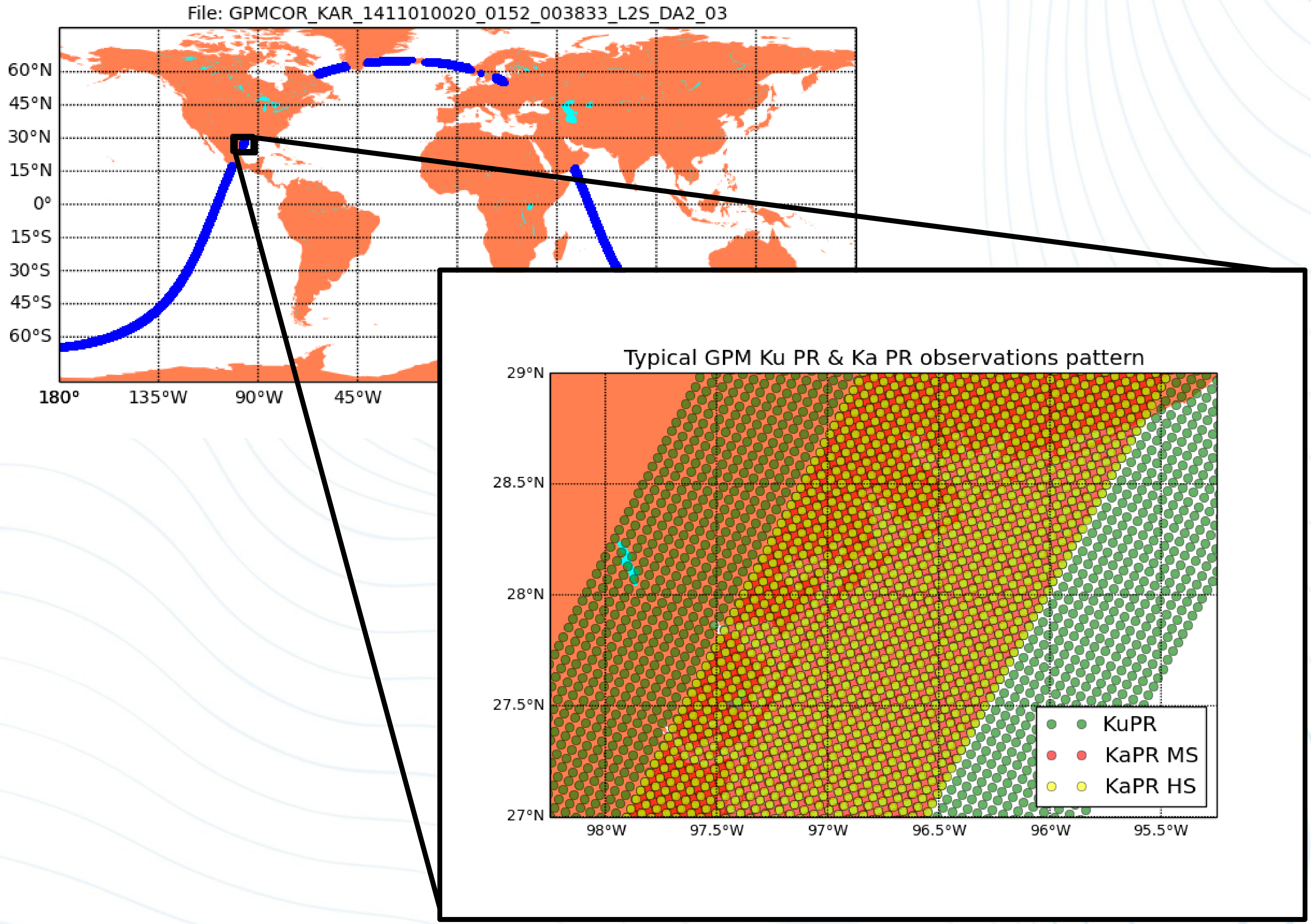

The GPM Mission: Coverage (benefits with respect to TRMM)

File: GPMCOR_KAR_1411010020_0152_003833_L2S_DA2_03

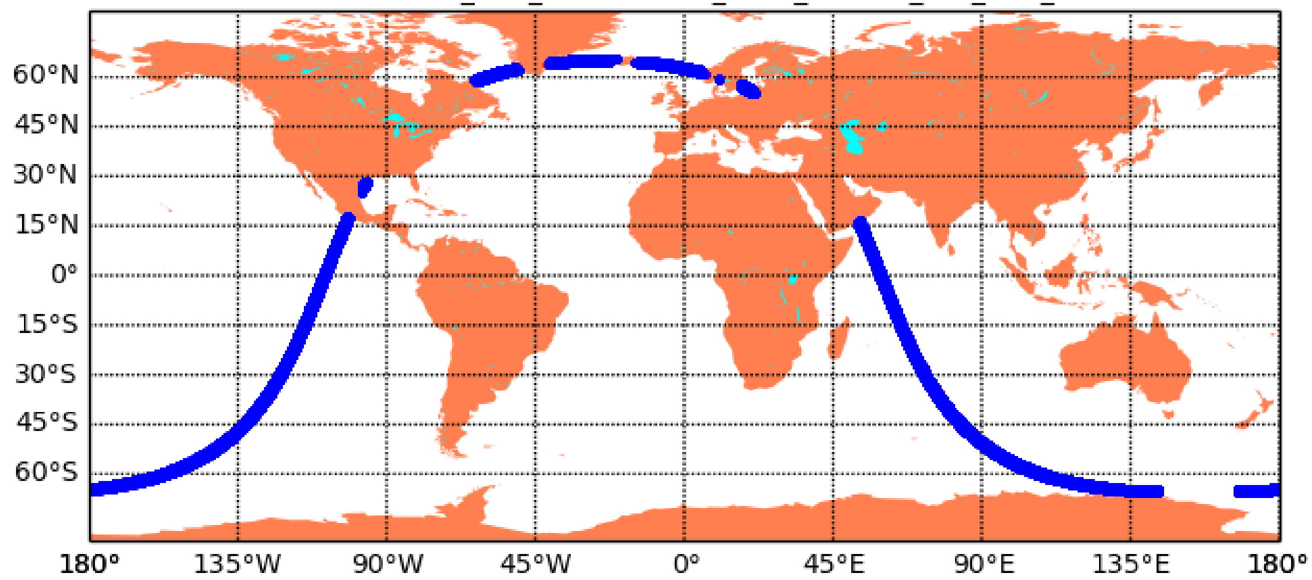

- Orbit has changed since TRMM.
- Latitudes larger than 30°N and 30°S are now observed by DPR. Acquisitions up to 66° north and south are now available.

- More chances to get extreme situations such as extra-tropical storms in high latitudes, with high winds and severe sea state.
- Area with strong ocean surface current such as Gulf Stream, Kuroshio or Agulhas current will be better covered.
- Opportunities to get sea ice, iceberg signature in Ka and Ku band at nea nadir.
- Acquisitions over Great lakes
- Co-existence with RapidSCAT & Sentinel-1 A

Analysis over Sea

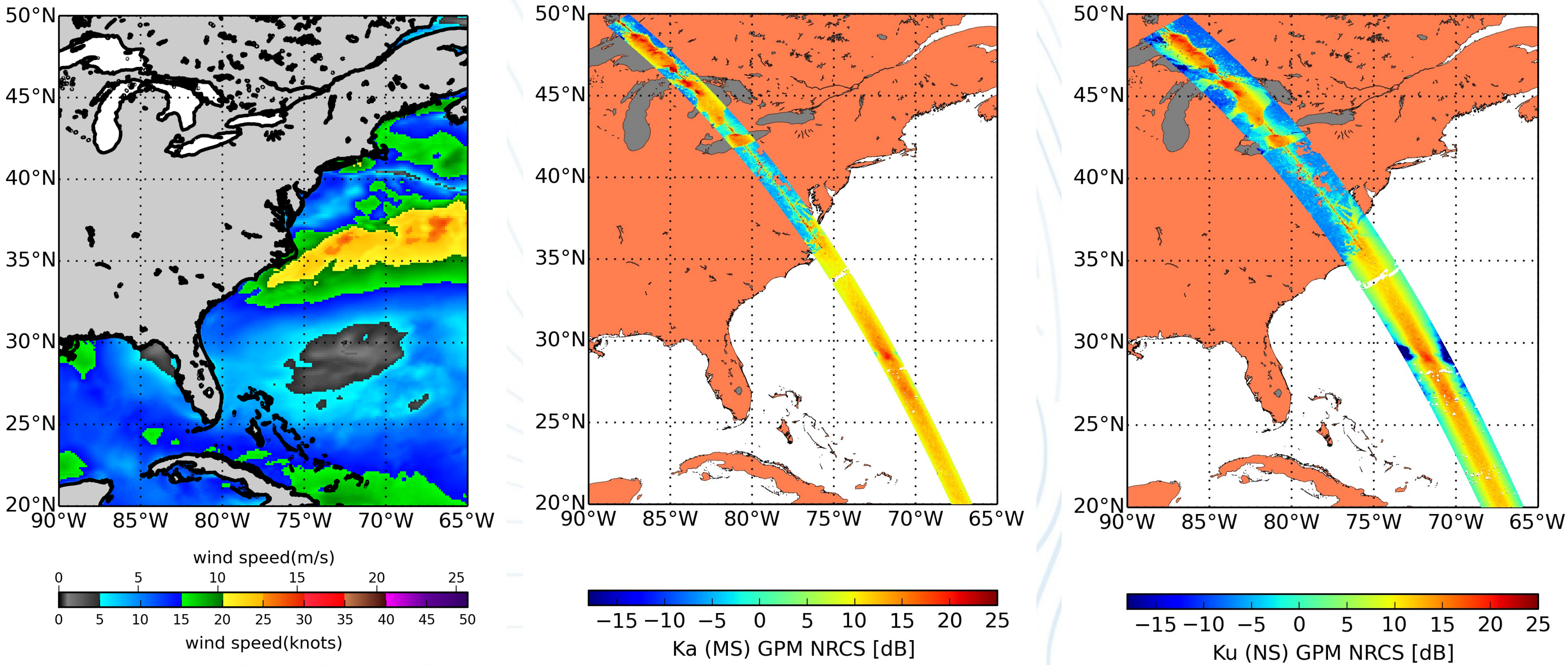

Exemple of acquisition in Ka (MS) and Ku (NS) Band with GPM over land, lake and Ocean

- Acquisitions over land can certainly help to prepare hydrology applications
- Consistency between NRCS acquired over ocean and ECMWF Winds

Analysis over Sea

Massive triple co-locations with Altika, WaveWatch 3 have been done to

- Compare the calibration between the two Ka-Band radar at nadir
- Check the dynamic of the signal

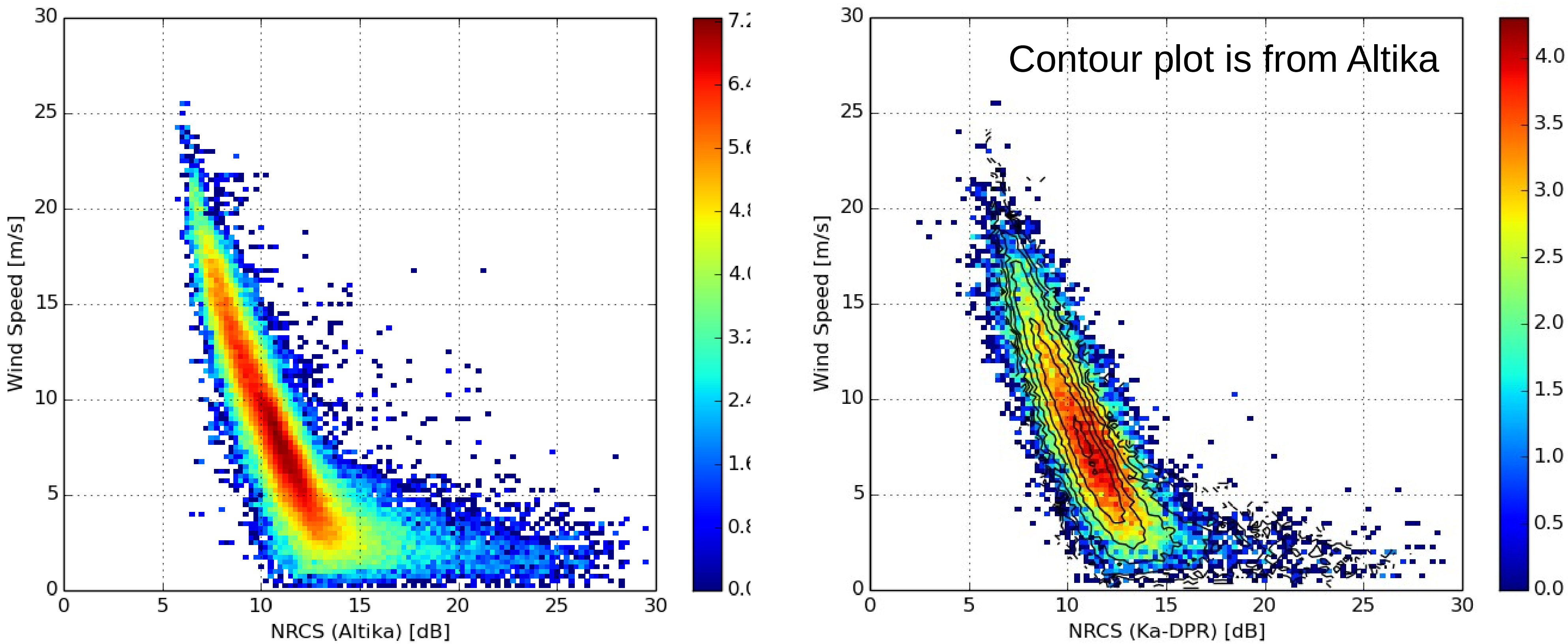

NRCS variations of Ka-DPR at nadir are very consistent with Altika
Bias is around 0.1 dB

Exemple of Acquisition over Sea Ice

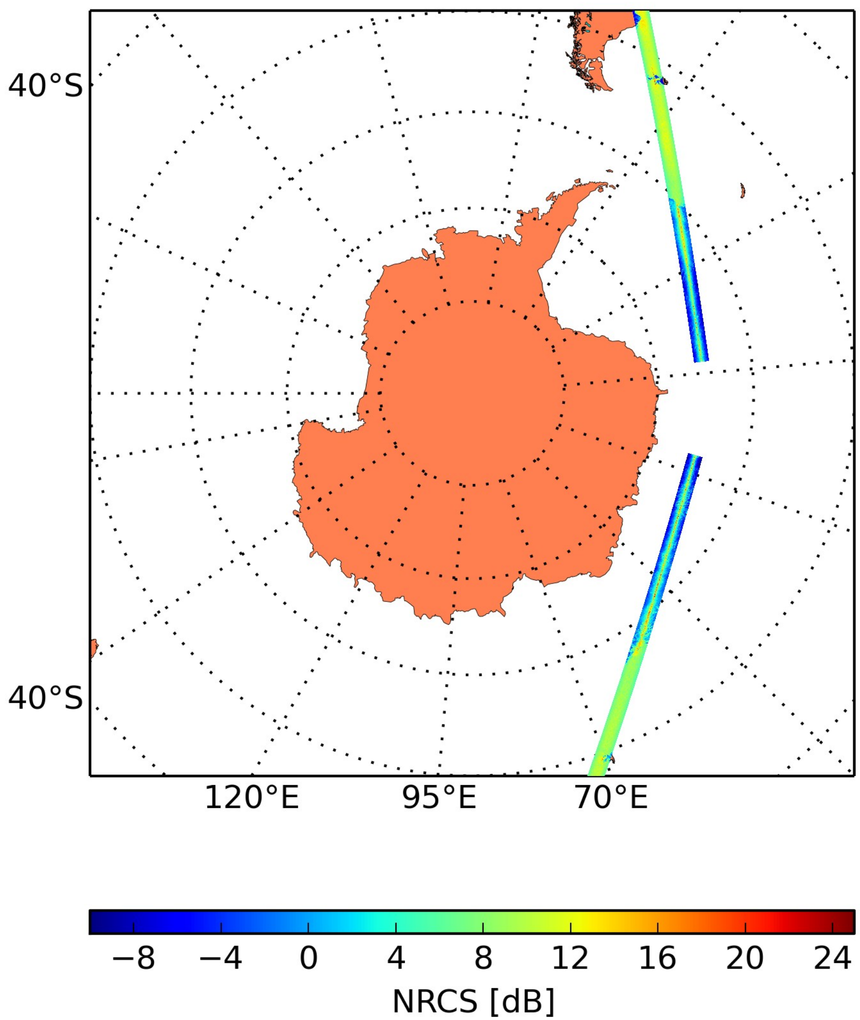

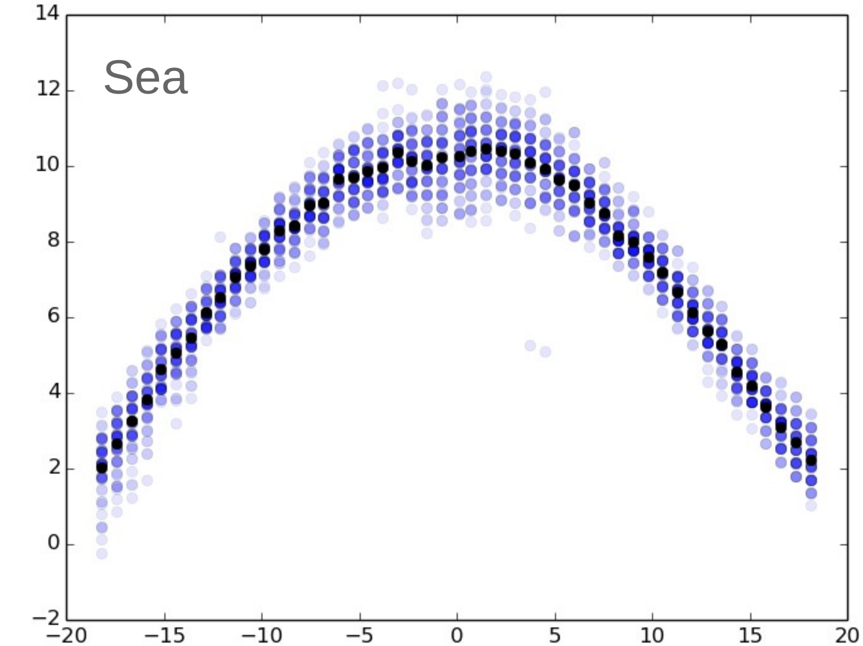

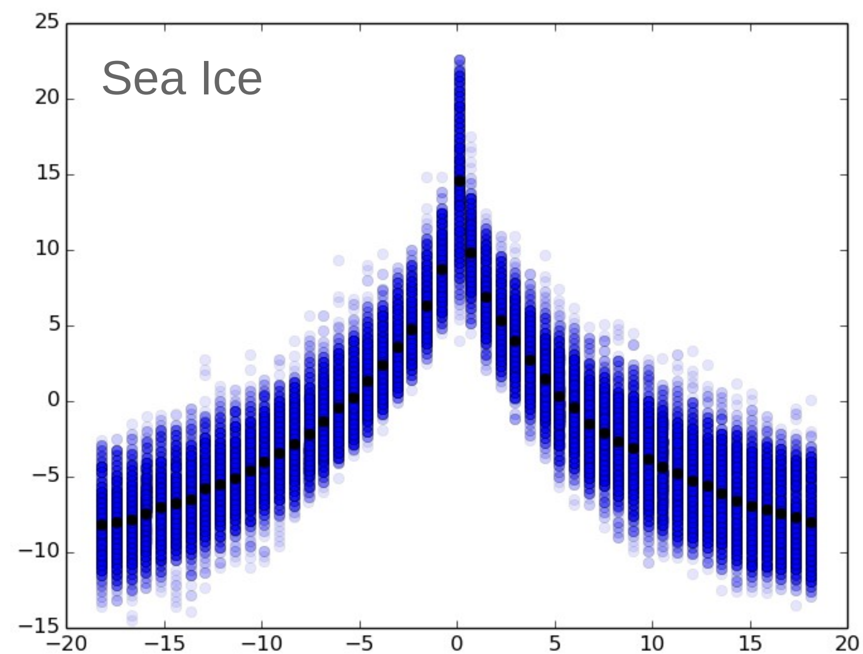

NRCS fall-off over sea ice is faster than over seas

Strong specular contribution for sea ice.

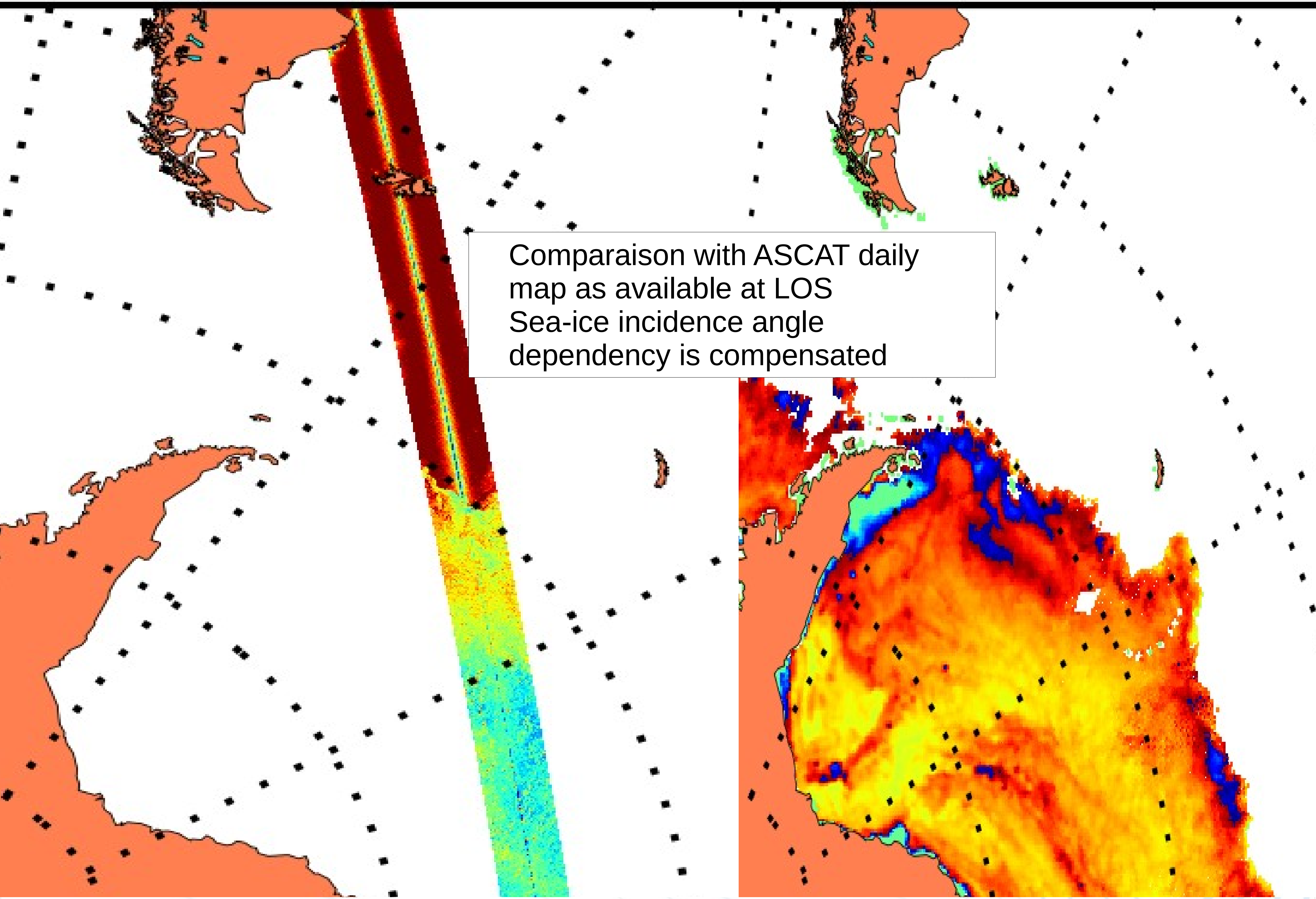

Comparaison with ASCAT daily map as available at LOS
Sea-ice incidence angle dependency is compensated

Monthly map of averaged NRCS as obtained in Ku-Band after detrend for September 2014

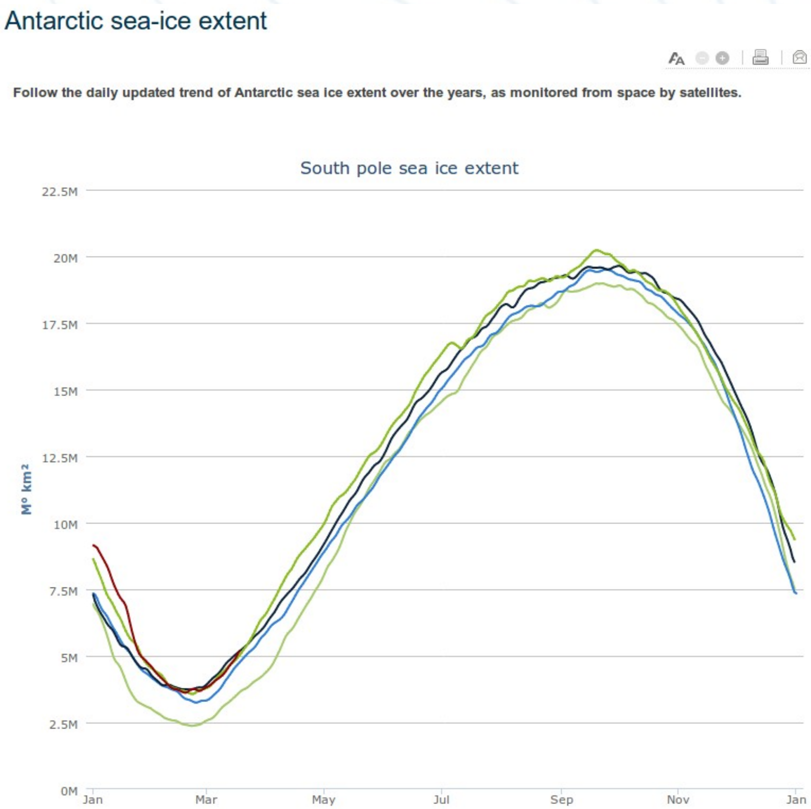

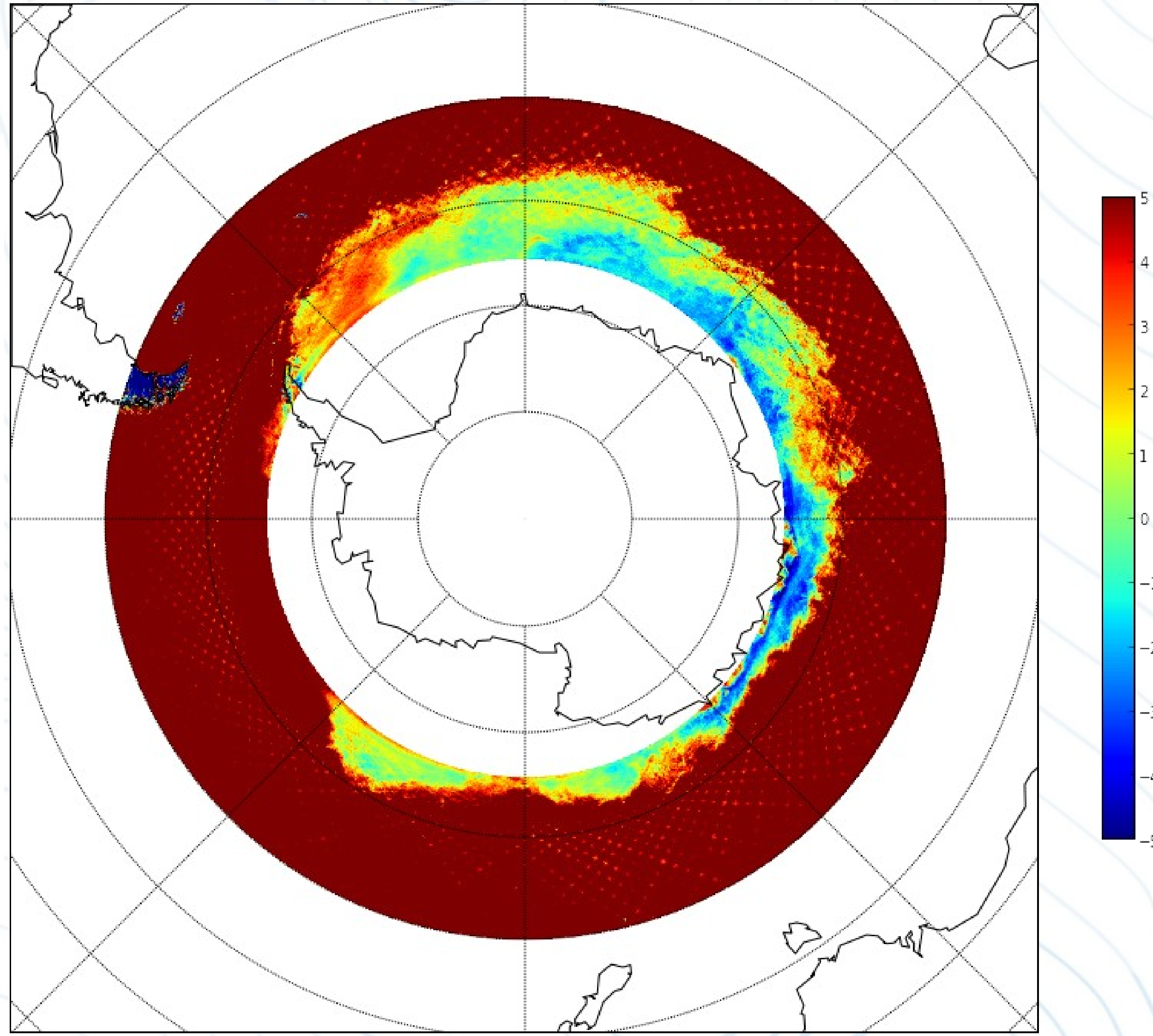

➡ Both sea ice-extent and NRCS spatial variability are observed in Ku and Ka-Band (not shown) at low incidence angles

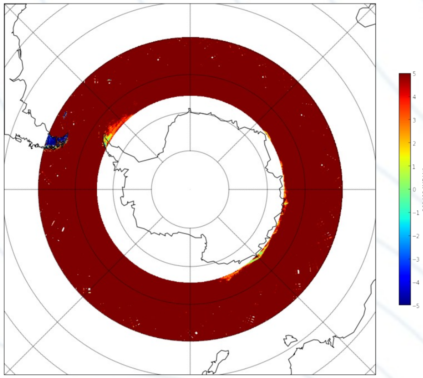
2014/03

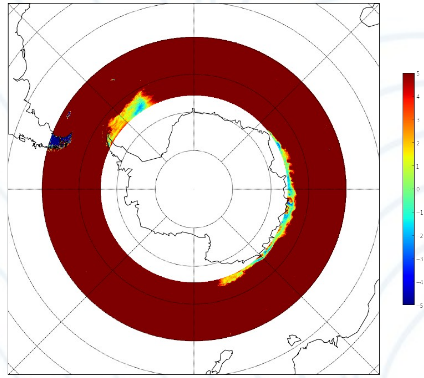
2014/04

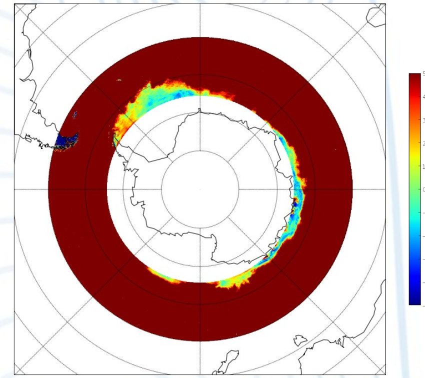
2014/05

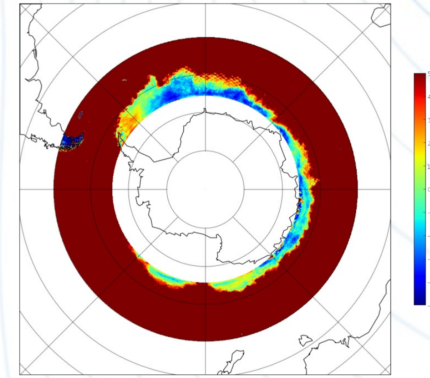
2014/06

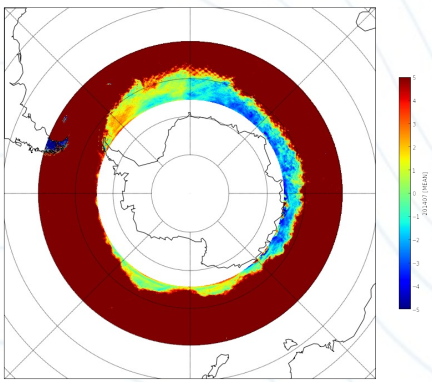
2014/07

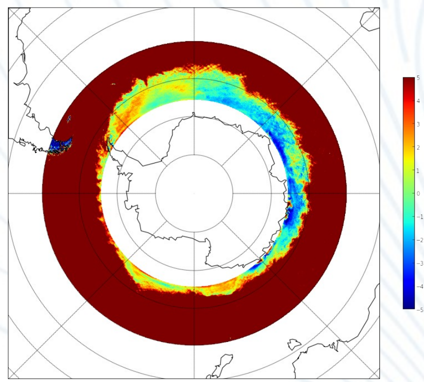
2014/08

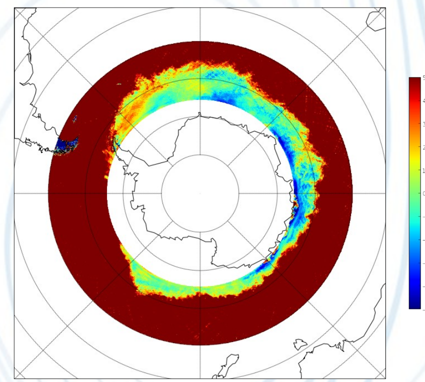
2014/09

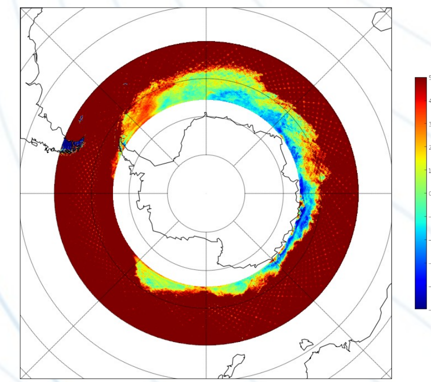
2014/10

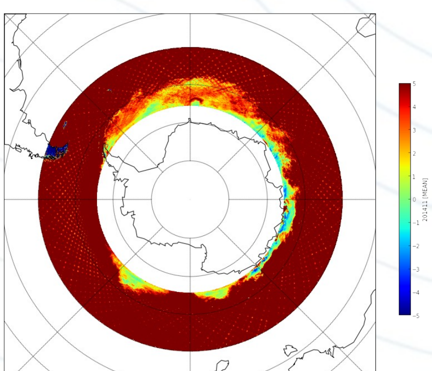
2014/11

Ku-Band Band maps along the year

Sea ice extent evolution and NRCS variability in space and time can be monitored with respect to time

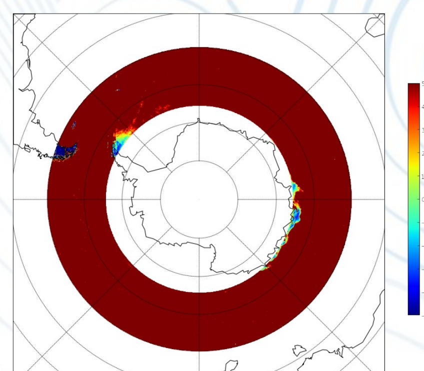
2015/01

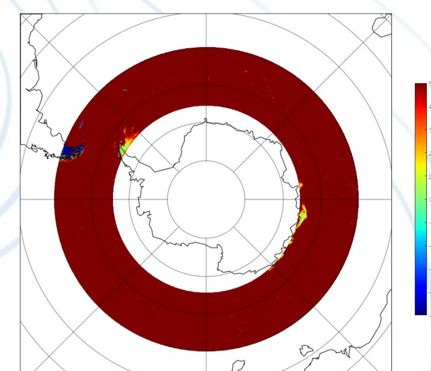
2015/02

Intercomparisons

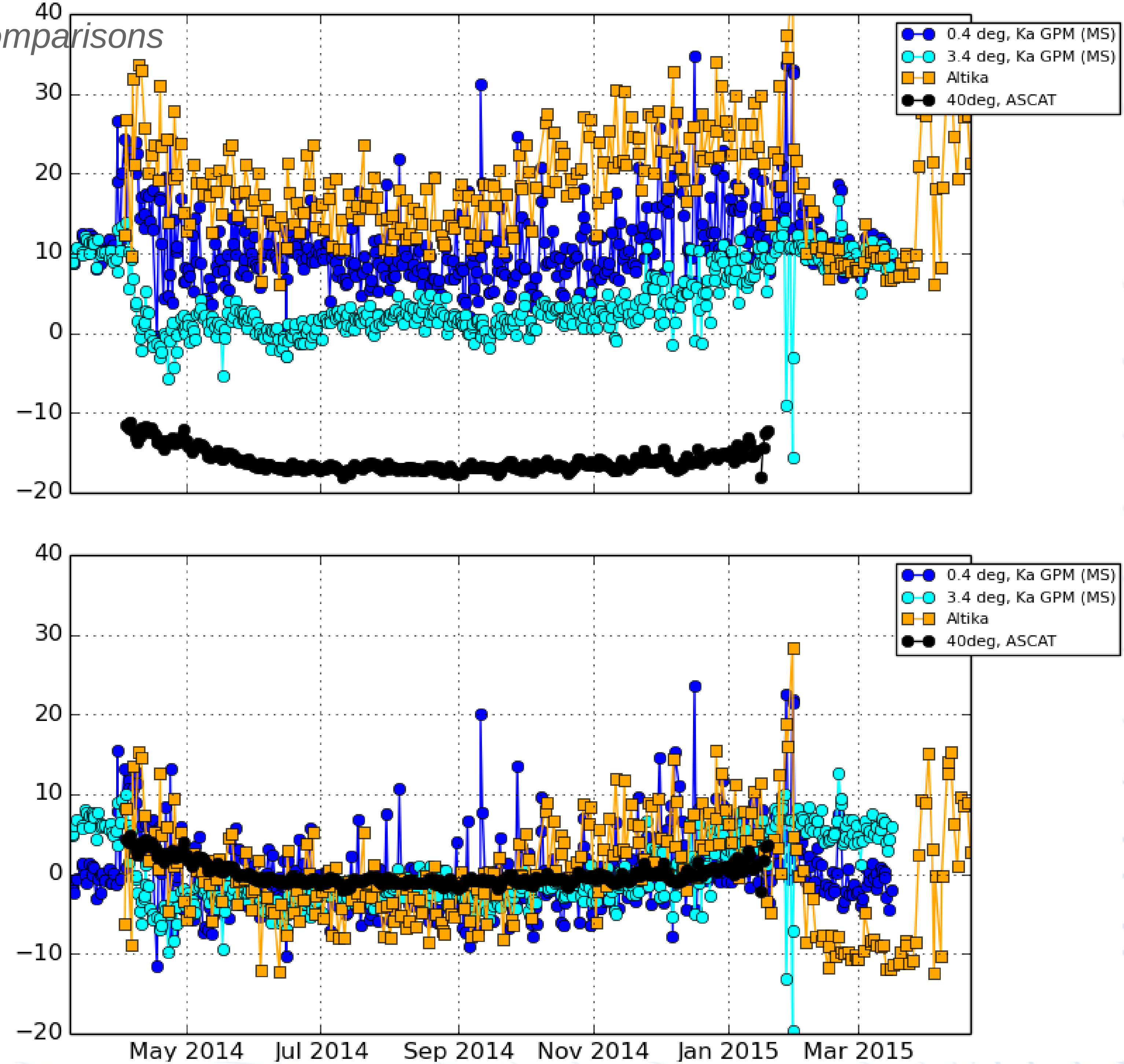

Inter-comparisons with ASCAT

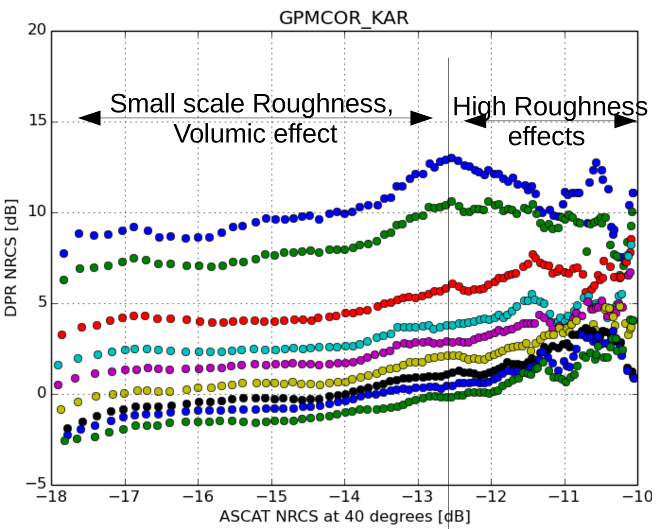

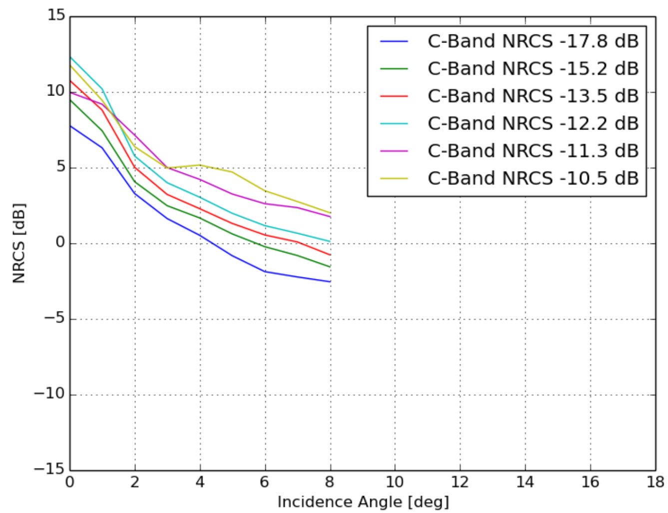

- Areas where NRCS$_{ascat}$ (40°) increases but remains below -12.5 dB (11.8 dB), the NRCS also increases at near-nadir.
- No changes are observed in the fall-off
  - It suggests an increase of the fraction of small scales roughness that contributes to backscattering
  - Or/And volumique scattering contribution from snow

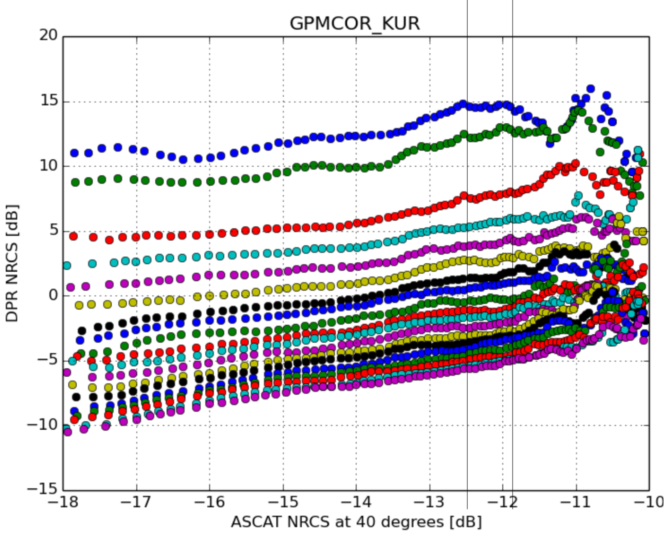

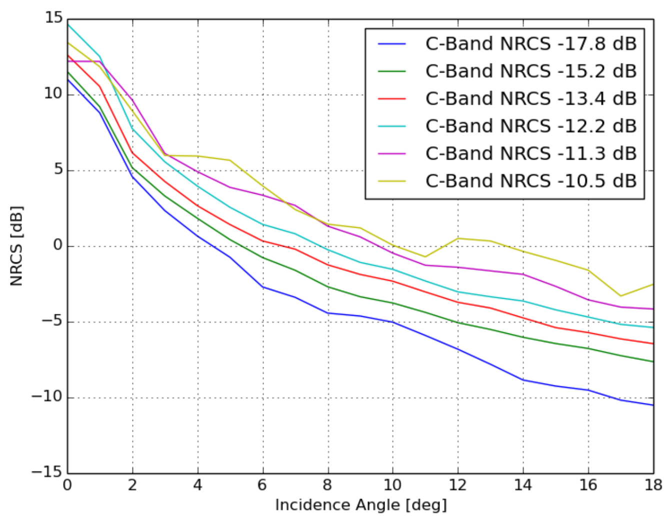

- Then for highest values of NRCS$_{ascat}$, the NRCS decreases at near-nadir.
- Changes are observed in the fall-off
  - It suggests apparition of roughness with steep slopes and wavelength larger than Bragg waves.

- More co-locations for high values of is NRCS$_{ascat}$ needed

NRCS variation as a function of time at Ka-Band

65°S,30°W

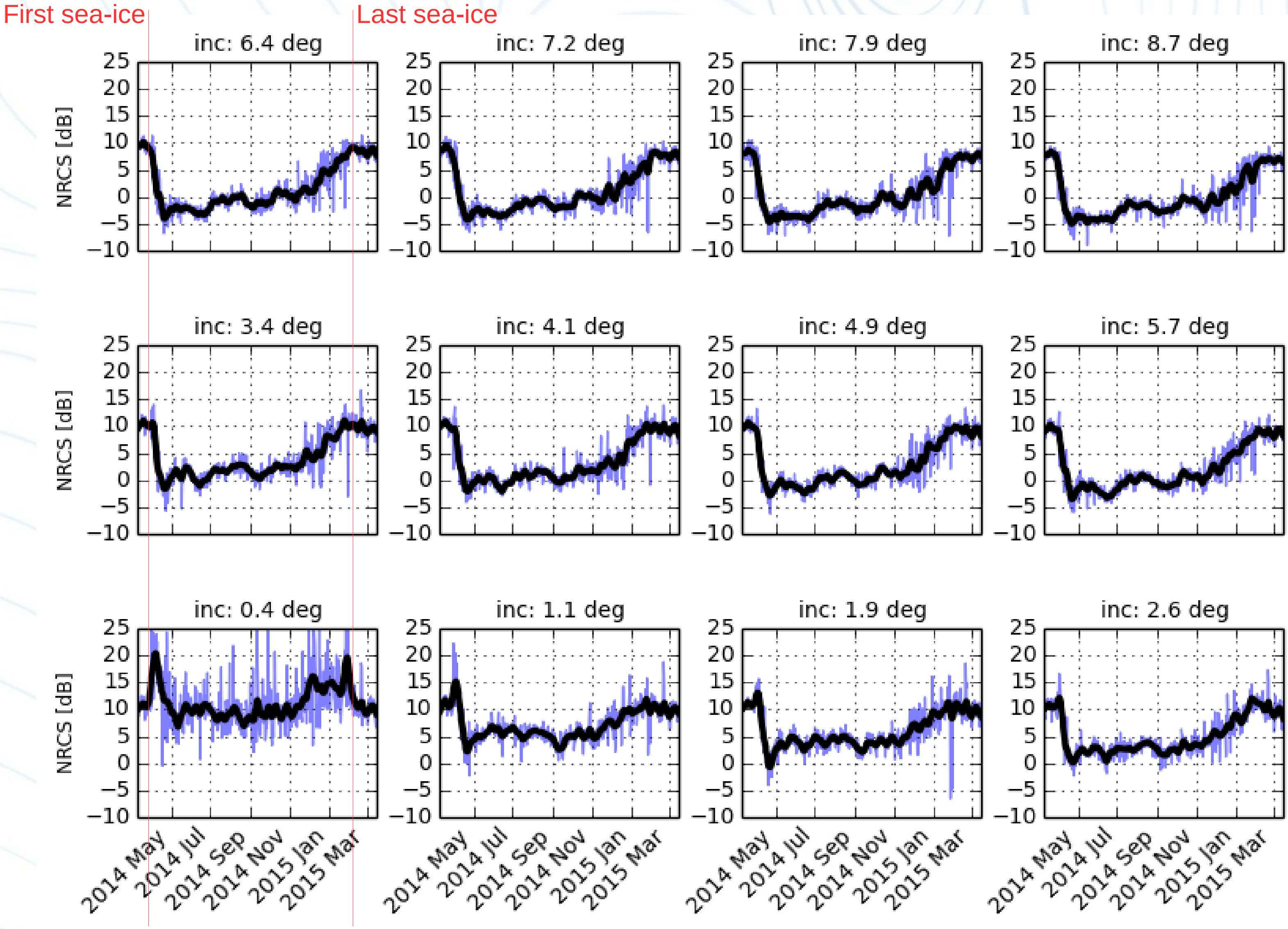

- Sensitivity is to specular contribution when sea ice starts to appear is very high for all incidences but different around nadir (increase) and after 2.6 degrees (decrease).
- Sensitivity to ice modifications (small variation of the NRCS) seems to increase from nadir to 5 degrees

NRCS fall-off variation as a function of time at Ka-Band

65°S,30°W

First sea-ice

Last sea-ice

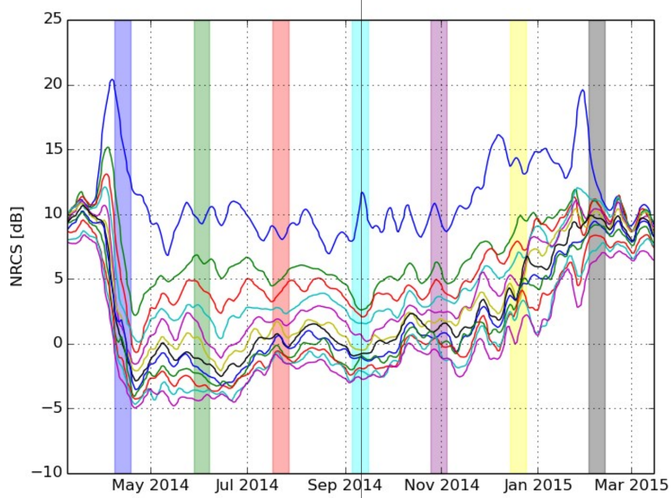

Maximum sea ice extent

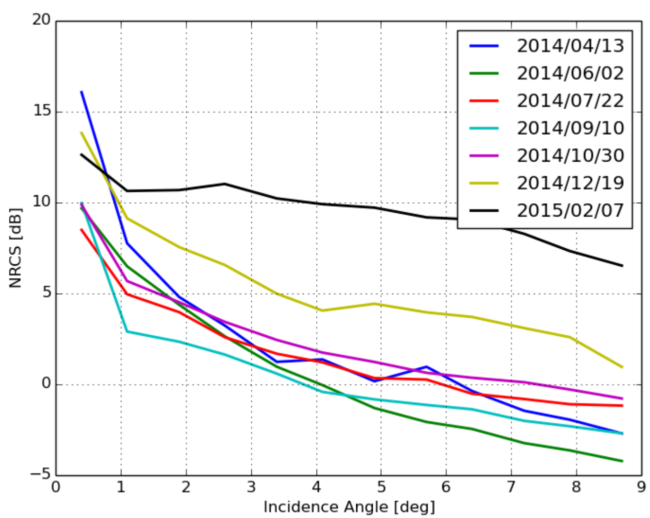

- At the beginning when sea ice starts to appear, the fall-off is very rapid. Sea ice can be assumed dry and flat. Electromagnetic waves and surface interactions are specular (blue line).
- During the period when the sea-ice extent increases, the specular contribution has decreased and the fall-off has no significant changes (green, red & cyan lines).
- After September, melting period starts
  - Just after September (cyan, magenta, yellow), the slope of the fall-off does not seem to change much. Only the level. It suggests a non incidence angle-dependent phenomena.
  - Then, just before total melting, the slopes is changing. It suggest apparition of roughness with steep slopes and wavelength larger than Bragg waves .